

Activation of IGF-1 and Insulin Signaling Pathways Ameliorate Mitochondrial Function and Energy Metabolism in Huntington's Disease Human Lymphoblasts

Luana Naia · I. Luísa Ferreira · Teresa Cunha-Oliveira · Ana I. Duarte · Márcio Ribeiro · Tatiana R. Rosenstock · Mário N. Laço · Maria J. Ribeiro · Catarina R. Oliveira · Frédéric Saudou · Sandrine Humbert · A. Cristina Rego

Received: 3 February 2014 / Accepted: 29 April 2014 / Published online: 20 May 2014
© Springer Science+Business Media New York 2014

Abstract Huntington's disease (HD) is an inherited neurodegenerative disease caused by a polyglutamine repeat expansion in the huntingtin protein. Mitochondrial dysfunction associated with energy failure plays an important role in this untreated pathology. In the present work, we used lymphoblasts obtained from HD patients or unaffected parentally related individuals to study the protective role of insulin-like growth factor 1 (IGF-1) versus insulin (at low nM) on signaling and metabolic and mitochondrial functions. Deregulation of intracellular signaling pathways linked to activation of insulin and IGF-1 receptors (IR, IGF-1R), Akt, and ERK was largely restored by IGF-1 and, at a less extent, by insulin in HD human lymphoblasts. Importantly, both neurotrophic

factors stimulated huntingtin phosphorylation at Ser421 in HD cells. IGF-1 and insulin also rescued energy levels in HD peripheral cells, as evaluated by increased ATP and phosphocreatine, and decreased lactate levels. Moreover, IGF-1 effectively ameliorated O₂ consumption and mitochondrial membrane potential ($\Delta\psi_m$) in HD lymphoblasts, which occurred concomitantly with increased levels of cytochrome c. Indeed, constitutive phosphorylation of huntingtin was able to restore the $\Delta\psi_m$ in lymphoblasts expressing an abnormal expansion of polyglutamines. HD lymphoblasts further exhibited increased intracellular Ca²⁺ levels before and after exposure to hydrogen peroxide (H₂O₂), and decreased mitochondrial Ca²⁺ accumulation, being the later recovered by IGF-1 and insulin in HD lymphoblasts pre-exposed to H₂O₂. In summary, the data support an important role for IR/IGF-1R mediated activation of signaling pathways and improved mitochondrial and metabolic function in HD human lymphoblasts.

L. Naia and I. L. Ferreira contributed equally for this study.

L. Naia · I. L. Ferreira · T. Cunha-Oliveira · A. I. Duarte · M. Ribeiro · T. R. Rosenstock · M. N. Laço · M. J. Ribeiro · C. R. Oliveira · A. C. Rego (✉)
CNC-Center for Neuroscience and Cell Biology, University of Coimbra, Largo Marquês de Pombal, 3004-517 Coimbra, Portugal
e-mail: a.cristina.rego@gmail.com

A. C. Rego
e-mail: arego@fmed.uc.pt

A. C. Rego
e-mail: acrego@cnc.uc.pt

L. Naia · M. N. Laço · C. R. Oliveira · A. C. Rego
Faculty of Medicine, University of Coimbra, Coimbra, Portugal

I. L. Ferreira · T. Cunha-Oliveira · A. I. Duarte · T. R. Rosenstock · M. N. Laço · C. R. Oliveira · A. C. Rego
Institute for Interdisciplinary Research, University of Coimbra (IIIUC), Polo II, Coimbra, Portugal

F. Saudou · S. Humbert
Institut Curie, Orsay 91405, France

Keywords Huntington's disease · Insulin · IGF-1 · Intracellular signaling · Mitochondria · Energy metabolism

Introduction

Huntington's disease (HD) is an autosomal progressive neurodegenerative disorder, characterized by an age-dependent loss in motor coordination, cognitive impairment, psychiatric disturbances and dementia, affecting about 10 in 10,000 individuals [1, 2]. HD neuropathology involves the selective death of striatal medium-sized spiny neurons due to an expansion of CAG repeats, encoding for a polyglutamine stretch at the N-terminus of the huntingtin (Htt) protein, which results in the formation of intranuclear aggregates [3, 4]. The current

hypothesis suggests that the disease arises from the combined effects of a gain of function in the mutated form of Htt (mHtt), along with a loss of function of wild-type Htt [5]. Despite these well-defined molecular alterations, many factors have been implicated in HD, including excitotoxicity, oxidative stress, alterations in Ca^{2+} handling, as well as a deregulation in transcription and intracellular signaling pathways [1, 6]. Importantly, impaired energy metabolism and mitochondrial function also play a central role in HD pathogenesis [7, 8]. Nevertheless, currently there is no neuroprotective treatment to prevent HD onset, disease progression, or patients' death.

Although HD affects mostly the central nervous system, growing evidence describes changes in peripheral tissues, such as lymphocytes [9], erythrocytes [10], fibroblasts [11], or platelets [12]. Abnormalities in weight loss and glucose homeostasis are also common clinical features among HD patients [13]. Furthermore, several studies in HD patients corroborated metabolic and mitochondrial dysfunction, showing (i) decreased mitochondrial complexes II, III, and IV activities in post-mortem brain samples and platelets [12, 14] and increased lactate levels in striatum and cortex [15]; (ii) reduced phosphocreatine/inorganic phosphate ratio in skeletal muscle [16]; and (iii) abnormal mitochondrial membrane potential in lymphoblasts [9, 11], and mitochondrial fragmentation in fibroblasts from HD patients [17]. In addition, previous studies performed in HD human cybrids (derived from HD human platelets) demonstrated an increase in mitochondrial Bim and Bak levels, and a slight release of cytochrome c, suggesting increased susceptibility to mitochondrial-dependent apoptosis [18]. More recent data evidenced mitochondrial dysfunction through decreased pyruvate dehydrogenase protein levels and activity, with consequent boosting of glycolysis in HD human cybrids [19], supporting bioenergetic disturbances in these cells.

Several studies have identified compounds that might be of therapeutic interest in HD. Neurotrophic factors such as insulin or insulin-like growth factor 1 (IGF-1) have been considered as potential therapeutic agents in neurodegenerative disorders [20, 21]. Previously, we demonstrated that insulin prevented the increase in both apoptotic and necrotic neuronal death associated with oxidative damage [22]. Moreover, insulin stimulated neuronal glucose uptake and subsequent metabolism into pyruvate, restoring intracellular ATP levels [23]. Besides regulating neuronal metabolism, insulin was shown to be neuroprotective against oxidative stress mediated by insulin receptor (IR)- and/or IGF-1 receptor (IGF-1R)-induced activation of phosphoinositide 3-kinase (PI3K)/Akt, inhibition of glycogen synthase kinase-3 β (GSK-3 β) [24] and forkhead box O1 (FoxO1) signaling pathways [25]. Other studies showed the beneficial effect of IGF-1, which regulates the size of neuronal populations during brain development [26, 27]. Moreover, the increase in IGF-1 and IGF-1R expression was associated to increased Akt (or protein kinase B) and

extracellular signal regulated kinase (ERK)1/2 phosphorylation [28]. Indeed, IGF-1 appears to be neuroprotective in the brain of ischemic rats, since it decreased neuronal apoptosis and improved motor function [29]. Furthermore, IGF-1 prevented neuronal death and protein aggregation induced by expression of mHtt; importantly, phosphorylation of Htt at Ser421 by Akt was shown to be essential for mediating this neuroprotective effect [21]. Recently, IGF-1 intranasal administration enhanced brain cortical IGF-1 levels and ameliorated Akt and Htt phosphorylation at Ser421, energy metabolic features, and motor function in YAC128 mice [30]. In addition, Pouladi et al. [31] described reduced IGF-1 expression in caudate and skin-derived fibroblasts from HD patients; moreover, proteomics profiling of plasma demonstrated that levels of the IGFBALS, a component of the IGF-1 ternary binding complex, are reduced in HD patients [32]. Conversely, Saleh et al. [33, 34] detected elevated plasma levels of IGF-1 associated with the severity of cognitive impairment in HD patients. Moreover, another study showed an increase in neuronal oxidative stress and mitochondrial dysfunction in transgenic R6/2 mice overexpressing insulin receptor substrate 2 (Irs2), a cytoplasmic molecule that mediates the effects of insulin and IGF-1 [35].

In light of these conflicting results, in this study, we explored how IGF-1 versus insulin (at low nM), acting through activation of IR, IGF-1R-mediated intracellular signaling, modulate HD-related mitochondrial and metabolic dysfunction, using human HD and family-related control lymphoblasts. This peripheral cell model derived from HD patients was previously shown to share several abnormalities related to mHtt, such as mitochondrial dysfunction, increased apoptosis, and transcriptional abnormalities [13]. Herein, we demonstrate reduced Akt and ERK activation and Htt phosphorylation, associated with reduced energy metabolism and mitochondrial dysfunction in HD human lymphoblasts, which are efficiently prevented by IGF-1 and, to a less extent, by insulin.

Material and Methods

Materials

Fetal bovine serum (FBS) and penicillin/streptomycin were from Gibco (Paisley, Scotland, UK). Insulin from porcine pancreas, IGF-1, glucose-6-phosphate, NADP, ADP, G6PDH, hexokinase, creatine kinase, protease inhibitor cocktail, oligomycin, CCCP, RPMI-1640 medium, and anti-tubulin were from Sigma Aldrich (St. Louis, MO, USA). enhanced chemifluorescence reagent, anti-rabbit IgG (from goat), and anti-mouse IgG+IgM (from goat) were from GE Healthcare (Little Chalfort, UK). Hoechst 33342, Alexa Fluor 488 goat anti-rabbit IgG, anti-complex (Cx) I (20 kDa) subunit, and anti-Cx IV (57 kDa) subunit were obtained from

Invitrogen (Carlsbad, CA, USA). Fura-2/AM, tetramethyl rhodamine methyl ester (TMRM⁺), MitoTracker Red CMXRos, anti-Cx I (30 kDa), and anti-Cx II (70 kDa) subunits were obtained from Molecular Probes/Invitrogen (Eugene, OR, USA). Lactate and pyruvate kits and anti-Tfam were from Abcam (Cambridge, UK). Amaxa cell line nucleofector Kit V was from Lonza (Basel, Switzerland). Bio-Rad Protein Assay was from Bio-Rad (Hemel Hempstead, UK). Anti-P-Akt (Ser473), anti-Akt, anti-p44/42 ERK (Thr202/Thr204), anti-p44/42 ERK, anti-IR/IGF-1R, anti-P-Foxo1 (Ser256), anti-Foxo1, anti-P-mTor (Ser2448), anti-mTor, anti-Bax, anti-p65, and anti-p53 were from Cell Signaling (Beverly, MA, USA). Polyvinylidene fluoride (PVDF) membrane and anti-P-IR/IGF-1R (Y1158/Y1162/Y1163) were from Millipore (Billerica, MA, USA). Anti-P-GSK-3 β (Tyr216), anti-GSK-3 β , anti-prohibitin, anti-TOM20, anti-TOM40 and anti-apoptosis-inducing factor (AIF) were from Santa Cruz Biotechnology (Santa Cruz, CA, USA). Anti-Hsp60 and anti-Htt (MAB1266) were obtained from Chemicon (Hampshire, UK). Anti-cytochrome c was from BD Biosciences Pharmingen (San Diego, CA, USA). Anti-P(Ser421)Htt was produced at Institute Curie (Orsay, France). Dako fluorescent mounting medium was from Palex Medical (Barcelona, Spain).

Cell Lines Culture and Treatment

Human lymphoblastoid cell lines, obtained from Coriell Institute for Medical Research (USA), were derived from HD-affected patients containing heterozygous expansion mutation, four males (43/15, 45/15, 42/18, and 49/17) and one female (47/18), or from unaffected voluntary control siblings, three males and one female, defined in this work as control (CTR) lymphoblasts. Lymphoblasts were maintained at a density of 400,000–600,000 cells/mL and cultured in RPMI-1640 medium supplemented with 15 % (v/v) non-inactivated FBS, 2 mM L-glutamine and 50 μ g/mL streptomycin plus 100 IU/mL penicillin in T25 or T75 flasks, in upright position, using an incubator chamber containing 5 % CO₂, 95 % air, and 100 % humidity, at 37°C. In these conditions, lymphoblastoid cell lines grow in suspension with cells clumped in loose aggregates. When used, these aggregates were dissociated by gently agitating the culture or by gentle trituration with a pipette. In 3–4 days, the cultures were either re-fed with fresh medium or split according to the rate of cell growth or the required number of cells needed for the experiments. For each experiment, HD or CTR cells were plated at 500,000 cells/mL in fresh RPMI medium and incubated for 24 h, in the absence (basal) or presence of 0.1 nM insulin or 0.1 nM IGF-1. For immunocytochemistry studies, lymphoblasts were left to adhere on poly-D-lysine glass coverslips (50,000 cells/cm²) for 1 h and then processed as described in “Fluorescence Imaging.”

Constructs and Transfection

The *wild-type* and polyQ-Htt constructs, 480-17Q, 480-68Q, 480-68-S421D, and 480-68-S421A, have been previously described [21]. CTR lymphoblasts were transiently transfected with 2 μ g plasmid DNA using Amaxa cell line nucleofector kit V 48 h before the experiment. Electroporation was carried out using the Lonza Nucleofector 2b device (Lonza, Switzerland) adjusted for E-032 program. Four hours after electroporation, RPMI medium was replaced by fresh medium to reduce the toxicity associated to the transfection medium.

Preparation of Total, Mitochondrial, and Cytosolic-Enriched Fractions and Western Blotting

HD and CTR lymphoblasts non-treated or treated with insulin or IGF-1 were centrifuged at 145 \times g, for 5 min, and washed with phosphate-buffered saline (PBS) solution containing (in mM): 137 NaCl, 2.7 KCl, 1.4 K₂HPO₄, and 4.3 KH₂PO₄, at pH 7.4.

Total Fractions Extracts were prepared in ice-cold lysis buffer (in mM: 20 Tris, 100 NaCl, 2 EDTA, 2 EGTA, 50 NaF, 1 Na₃VO₄, 1 % Triton; pH 7.4) supplemented with 1 mM 1,4-dithiothreitol (DTT), 100 μ M phenylmethylsulfonyl fluoride (PMSF), 100 nM okadaic acid and 1 μ g/mL protease inhibitor cocktail (chymostatin, pepstatin A, leupeptin, and antipain). The homogenates (total fractions) were then frozen/thawed three times in liquid nitrogen and centrifuged at 20,800 \times g for 10 min (4°C) in order to remove cell debris; the resulting supernatant was collected and stored at 80 °C for later use.

Mitochondrial and Cytosolic-Enriched Fractions Cells were re-suspended in ice-cold sucrose buffer (in mM: 250 sucrose, 20 HEPES/KOH (pH 7.5), 100 KCl, 1.5 MgCl₂, 1 EGTA, and 1 EDTA), supplemented with 1 mM DTT, 100 μ M PMSF, 100 nM okadaic acid, and 1 μ g/mL protease inhibitor cocktail. Lysates, obtained after homogenization, were centrifuged at 560 \times g for 12 min (4 °C) to pellet the nuclei and cell debris. The supernatant was further centrifuged at 12,000 \times g for 20 min (4 °C) and the resulting pellet (mitochondrial-enriched fraction) resuspended in supplemented sucrose buffer. TCA (15 %) was added to the supernatant, and precipitated proteins were centrifuged at 16,300 \times g for 10 min (4 °C). The resulting pellet (cytosolic-enriched protein fraction) was re-suspended in supplemented sucrose buffer and brought to pH 7 with KOH (as in [36]). Both fractions were stored at 80 °C for later use.

For Western blotting, equivalent amounts of protein were subjected to sodium dodecyl sulfate polyacrylamide gel electrophoresis (SDS-PAGE) gel (10 or 12 %), transferred onto

PVDF membranes, and incubated for phosphorylated proteins with anti-P-Akt (Ser473) (1:1,000), P-p44/42 ERK (Thr202/Tyr204) (1:1,000), P(Tyr1158/Tyr1162/Tyr1163)-IR/IGF-1R (1:1,000), P-GSK-3 β (Tyr216) (1:500), P-mTor (Ser2448) (1:1,000), P-Foxo1 (Ser256) (1:500), and P-Htt (Ser421) (1:200) antibodies. These phosphorylated proteins were further normalized using the following antibodies: Akt (1:1,000), p44/42 ERK (1:1,000), IR/IGF-1R (1:1,000), GSK-3 β (1:500), mTor (1:1000), Foxo1 (1:750), and Htt(MAB2166) (1:250). For analysis of total proteins, membranes were incubated with TOM20 (1:200), TOM40 (1:500), prohibitin (1:2,000), Tfam (1:1,000), Bax (1:1,000), p65 (1:500), p53 (1:2,000), AIF (1:1,000), and cytochrome c (1:500) antibodies, overnight at 4°C. These proteins were normalized using anti-tubulin (1:20,000) or Hsp60 (1:1,000) antibodies. Membranes were then incubated with anti-rabbit IgG and anti-mouse IgG+IgM secondary antibodies (1:20,000), for 90 min at room temperature, and immunoreactive bands visualized using VersaDoc Imaging System (BioRad, Hercules, USA). Fluorescence signal was analyzed using the QuantityOne software, and the results were given as percentage of control.

Measurement of Intracellular Accumulation of Adenine Nucleotides, Phosphocreatine and Pyruvate Levels

HD or CTR lymphoblasts, treated or not with insulin or IGF-1, were washed with ice-cold PBS and centrifuged at 145 \times g, for 5 min (4°C). Extracts were performed with 0.6 M perchloric acid supplemented with 25 mM EDTA-Na⁺ and then centrifuged at 20,800 \times g for 2 min at 4 °C to remove cell debris. The resulting pellet was solubilized with 1 M NaOH and further analyzed for total protein content by the Bio-Rad Protein assay. After neutralization with 3 M KOH/1.5 M Tris, samples were centrifuged at 20,800 \times g for 5 min, at 4 °C. The resulting supernatants were assayed for:

1. ATP, ADP, and AMP determination by separation in a reverse-phase high-performance liquid chromatography, with detection at 254 nm, as described previously [37]. The chromatographic apparatus used was a Beckman-System Gold controlled by a computer. The detection wavelength was 254 nm, and the column used was a Lichrospher 100 RP-18 (5 μ m). An isocratic elution with 100 mM phosphate buffer (KH₂PO₄), pH 6.5, and 1 % methanol was performed with a flow rate of 1 mL/min. Peak identity was determined by following the retention time of standards.
2. Intracellular phosphocreatine levels, by following NADP⁺ reduction at 339 nm, mediated by ATP production by creatine kinase, in the presence of hexokinase and glucose-6-phosphate dehydrogenase (G6PD), using a Microplate Spectrophotometer SpectraMax Plus 384

(Molecular Devices, USA), according to a previously described method [38]. The results were expressed in picomole phosphocreatine/milligram protein.

3. Intracellular pyruvate levels using the Pyruvate Assay Kit (Abcam). In this assay, pyruvate is oxidized by pyruvate oxidase, further generating a fluorescent compound. The fluorescence was measured by fluorimetry ($E_x/E_m=535/587$ nm), and the intensity was proportional to pyruvate content.

Assessment of Intracellular Lactate

Treated or untreated HD and CTR lymphoblasts were washed with ice-cold PBS and extracted with 0.6 M perchloric acid supplemented with 25 mM EDTA-Na⁺. Cell extracts were centrifuged at 20,800 \times g for 5 min at 4 °C to remove cell debris (as in [18]). Intracellular lactate levels were determined using the Lactate Assay Kit (Abcam). In this assay, lactate is oxidized by lactate dehydrogenase to generate pyruvate and NADH, which in turn reacts with WST to produce a colored product (formazan; OD=450 nm).

O₂ Consumption

HD or CTR lymphoblasts, incubated in the absence or in the presence of 0.1 nM insulin or 0.1 nM IGF-1, were washed and re-suspended in Krebs buffer containing (in mM): 132 NaCl, 4 KCl, 1 CaCl₂, 1.2 NaH₂PO₄, 1.4 mM MgCl₂, 6 glucose, 10 HEPES, and aliquots containing 5 \times 10⁶ cells placed in an oxygen electrode chamber (DW1, Clark electrode, Hansatech, UK), after calibration for dissolved oxygen. After recording the basal rate of oxygen consumption (in nmol mL⁻¹ min⁻¹), maximum respiration was assessed by adding 2.5 μ M carbonyl cyanide 3-chlorophenylhydrazone (CCCP) plus 2 μ g/mL oligomycin to the reaction medium. KCN (700 μ M) was added at the end of the experiment to confirm O₂ consumption by mitochondria.

Assay of Enzymatic Activities of Mitochondrial Electron Transport Chain

Mitochondrial crude fractions prepared from treated versus non-treated HD or CTR lymphoblasts were obtained as described in “[Preparation of Total, Mitochondrial, and Cytosolic-Enriched Fractions and Western Blotting](#)” (without supplementation with DTT, PMSF, or protease inhibitor cocktail) and used for further analysis of enzymatic activities of mitochondrial electron transport chain complexes.

NADH-Ubiquinone Oxidoreductase Assay Complex I activity was determined at 340 nm by following the decrease in NADH absorbance due to ubiquinone reduction to ubiquinol

[39]. Complex I activity was expressed in nanomoles per minute per milligram protein and corresponds to the rotenone sensitive rate.

Succinate–Ubiquinone Oxidoreductase Assay Complex II activity was monitored at 600 nm by following the reduction of 6,6-dichlorophenolindophenol (DCPIP) by the ubiquinol resulting from this reaction [40]. Complex II activity was expressed in nanomoles per minute per milligram protein and corresponds to the thenoyltrifluoroacetone (TTFA) sensitive rate.

Ubiquinol–Cytochrome C Reductase Assay Complex III activity was monitored at 550 nm by following the ubiquinol reduction of cytochrome c. The assay was started by adding the sample to the reaction mixture (in mM: 35 K₂HPO₄, pH 7.2, 1 EDTA, 5 MgCl₂, 1 KCN, 5 μM rotenone) containing 15 μM cytochrome c and 15 μM ubiquinol, at 30°C. Complex III activity was expressed in rate constant (*k*) per minute per milligram of protein.

Cytochrome c Oxidase Assay Complex IV activity was determined at 550 nm by measuring the oxidation of reduced cytochrome c by cytochrome c oxidase [41]. Complex IV activity was expressed in rate constant (*k*) per minute per milligram of protein.

All enzyme activity was corrected for citrate synthase (CS) activity. For citrate synthase assay, CS activity was performed at 412 nm following the reduction of 5,5'-dithio-bis(2-nitrobenzoic acid) in the presence of acetyl-CoA and oxaloacetate [42]. CS activity was expressed in nanomoles per minute per milligram protein.

TMRM⁺ Fluorescence

Mitochondrial membrane potential was assessed using the cationic fluorescent probe TMRM⁺, which accumulates predominantly in polarized mitochondria. Thus, the variation of TMRM⁺ retention was studied in order to estimate changes in mitochondrial membrane potential. Following a washing step, HD or CTR lymphoblasts, treated or not with insulin or IGF-1, were incubated in Krebs medium containing 300 nM TMRM⁺ (quench mode) for 1 h at 37 °C. Basal fluorescence (540 nm excitation and 590 nm emission) was measured using a microplate reader Spectrofluorometer Gemini EM (Molecular Devices, USA), for 4 min, followed by the addition of 2.5 μM CCCP plus 2 μg/mL oligomycin to produce maximal mitochondrial depolarization.

Intracellular Ca²⁺ Recordings

HD or CTR lymphoblasts, incubated in the absence or in the presence of 0.1 nM insulin or 0.1 nM IGF-1, were incubated

in Krebs medium containing the fluorescent probe Fura-2/AM (10 μM) in the incubator chamber, at 37°C, for 30 min. After a washing step, intracellular Ca²⁺ levels were measured in basal conditions or in response to 1 mM hydrogen peroxide (H₂O₂) and/or 2 μM CCCP plus 2 μg/mL oligomycin, using a Spectrofluorometer Gemini EM (Molecular Devices, USA), with 340/380 nm excitation and 510-nm emission wavelengths.

Fluorescence Imaging

HD or CTR lymphoblasts, incubated in the absence or presence of 0.1 nM insulin or 0.1 nM IGF-1, and further adhered to glass coverslips, as described in “Cell Lines Culture and Treatment,” were exposed to 500 nM MitoTracker Red CMXRos (MtT Red) in Krebs medium during 40 min, at 37°C. Cells were fixed with 4 % paraformaldehyde for 20 min and then permeabilized with 0.2 % (v/v) Triton X-100 in PBS. After a washing step, cells were blocked with 3 % (w/v) bovine serum albumin and then incubated with TOM-20 (1:200) primary antibody and further with anti-mouse Alexa Fluor 488 (1:200) secondary antibody. Finally, the coverslips were mounted using Dako fluorescent mounting medium and examined using a Zeiss LSM S10 META confocal microscope (Carl Zeiss, Oberkochen, Germany) equipped with a 63x/1.4 Plan-ApoChromat objective. The lasers used were argon/2 (488 nm) and DPSS 561-10 (561 nm). The acquisition of images was performed in the LSM 510 software.

Data Analysis and Statistics

Data were expressed as the mean±SEM of the number of experiments indicated in the figure legends. Comparisons among multiple groups were performed by two-way ANOVA, followed by Bonferroni post hoc test. Student's *t* test was also performed for comparison between two Gaussian populations, as described in figure legends. Significance was accepted at *p*<0.05.

Results

IGF-1 Stimulates Akt and ERK Signaling Pathways

In previous studies, Akt was shown to be downregulated through cleavage by caspase-3 in both animal models and HD patients at late stages of the disease [43]. This was associated with a deregulation of IGF-1/Akt signaling pathway caused by mHtt along the course of the disease [21]. Using lymphoblasts cell lines derived from HD patients and control siblings, we evaluated the insulin/IGF-1 signaling pathways. Our results demonstrate that IR, IGF-1R phosphorylation at Tyr1158, 1162, and 1163, previously described to

reflect their activation [24, 44], was significantly decreased in HD patient's lymphoblasts (Fig. 1a*i*), whereas no significant changes were observed in IR,IGF-1R protein levels (Fig. 1a, *ii*). Exposure to IGF-1 (0.1 nM) enhanced IR,IGF-1R activation in HD cells by about 2-fold, whereas no changes in IR,IGF-1R activation were observed in the presence of insulin (0.1 nM). In addition, we found a significant decrease in Akt and ERK42/44 phosphorylation in HD lymphoblasts, which were prevented by insulin and IGF-1 (Fig. 1b, *i*, *iii* and *c*, *i*, *iii*), suggesting an activation of PI3K/Akt and Ras/ERK signaling pathways in HD human lymphoblasts subjected to insulin and, particularly, IGF-1 treatment. Importantly, at IR, the rank order of affinity to insulin (~1 nM)>>IGF-1 (100–500-fold), whereas at IGF-1R IGF-1 (~1 nM)>>insulin (100–500-fold)

[45]. Therefore, low nanomolar concentrations of insulin and IGF-1 may activate each receptor subtype.

Given the decrease in Akt activation in HD lymphoblasts, we measured phosphorylated and total levels of Akt downstream proteins. Mammalian target of rapamycin (mTor) total protein levels were significantly decreased in HD cells, by about 50 %, compared to the CTR (Fig. 1d, *ii*). Interestingly, mTor activation was significantly increased in HD lymphoblasts (by 155 %, Fig. 1d, *i*), but further exposure to insulin or IGF-1 had no significant additional effect. Moreover, no significant differences were observed in Foxo-1 Ser256 phosphorylation, a target of Akt (Fig. 1e). In addition, the Ser/Thr kinase GSK-3 β , which has the potential to modulate blood glucose levels [46], was not altered in HD lymphoblasts.

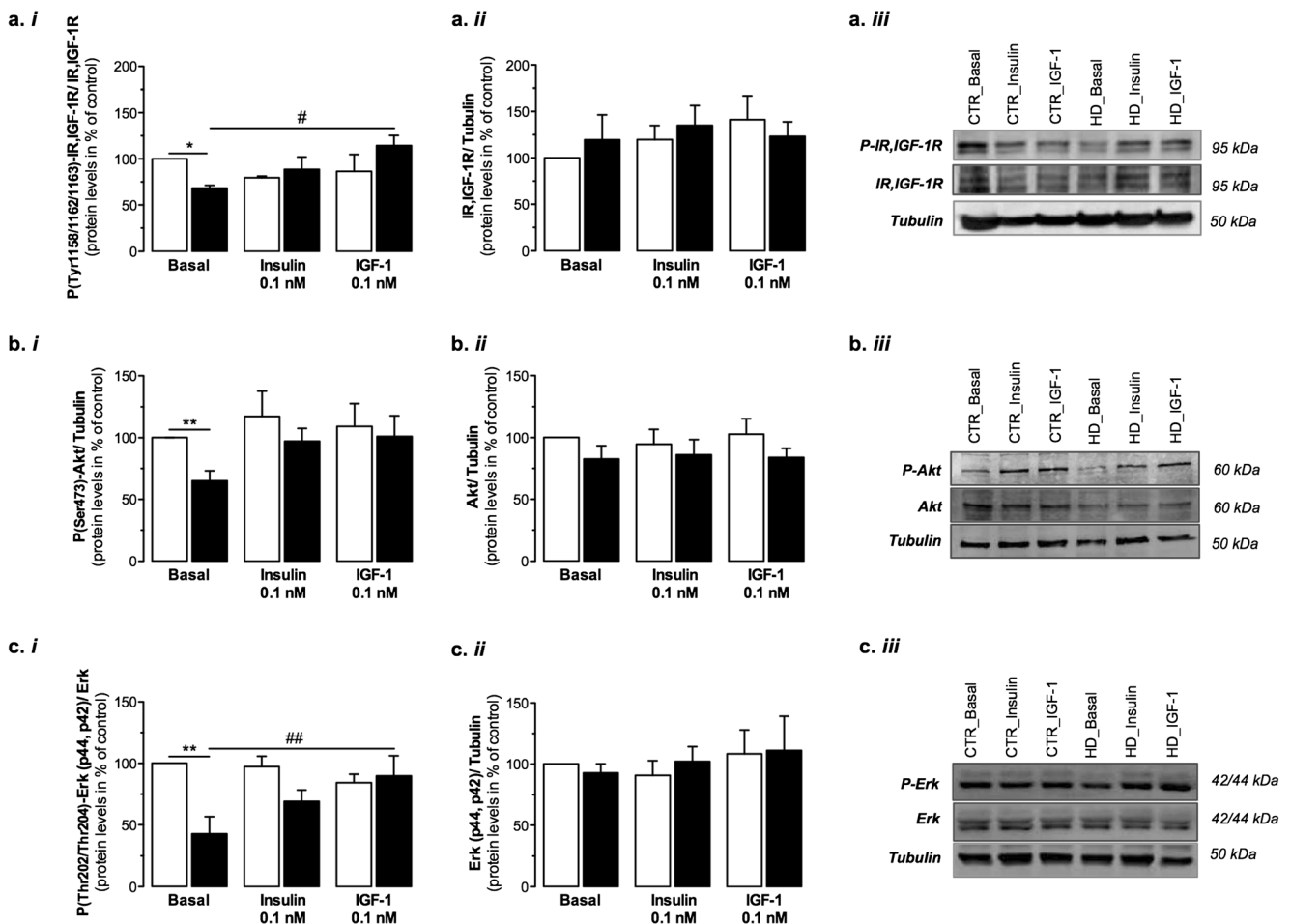


Fig. 1 IGF-1 and insulin mediated activation of IR,IGF-1R signaling pathways. CTR or HD lymphoblasts were untreated (basal) or treated with 0.1 nM insulin or IGF-1 in culture medium (RPMI-1640) for 24 h at 37°C. Total cell lysates were electrophoresed on 10 % SDS-PAGE and probed for phosphorylated proteins with anti-P(Y1158/Y1162/Y1163)-IR,IGF-1R (**a**, *i*), anti-P(Ser473)-Akt (**b**, *i*), anti-P(Thr202/Thr204)-ERK (**c**, *i*), anti-P(Ser2448)-mTor (**d**, *i*), anti-P(Ser256)-Foxo1 (**e**, *i*), and anti-P(Tyr216)-GSK3 β (**f**, *i*) selective antibodies, followed by reprobing for total protein with anti-IR,IGF-1R (**a**, *ii*), anti-Akt (**b**, *ii*), anti-ERK (**c**, *ii*), anti-mTor (**d**, *ii*), anti-FOXO1 (**e**, *ii*), and anti-GSK3 β (**f**, *ii*) selective

antibodies. All total proteins were normalized with anti-tubulin antibody. Data are the mean \pm SEM from three to six independent experiments, expressed as percentage of CTR (under basal conditions), considering 0.59 \pm 0.01 (**a**, *i*), 0.32 \pm 0.04 (**a**, *ii*), 0.57 \pm 0.28 (**b**, *i*), 1.36 \pm 0.37 (**b**, *ii*), 5.59 \pm 2.41 (**c**, *i*), 0.08 \pm 0.04 (**c**, *ii*), 0.55 \pm 0.11 (**d**, *i*), 1.88 \pm 0.74 (**d**, *ii*), 1.62 \pm 0.49 (**e**, *i*), 0.91 \pm 0.34 (**e**, *ii*), 2.24 \pm 0.39 (**f**, *i*), and 0.11 \pm 0.02 (**f**, *ii*) INT/mm² as 100 %. Statistical analysis: ^t P <0.05, ^{tt} P <0.01 vs respective CTR (Student's *t* test); * P <0.05, ** P <0.01 vs respective CTR; # P <0.05, ### P <0.01 vs untreated HD (two-way ANOVA, followed by Bonferroni post hoc test)

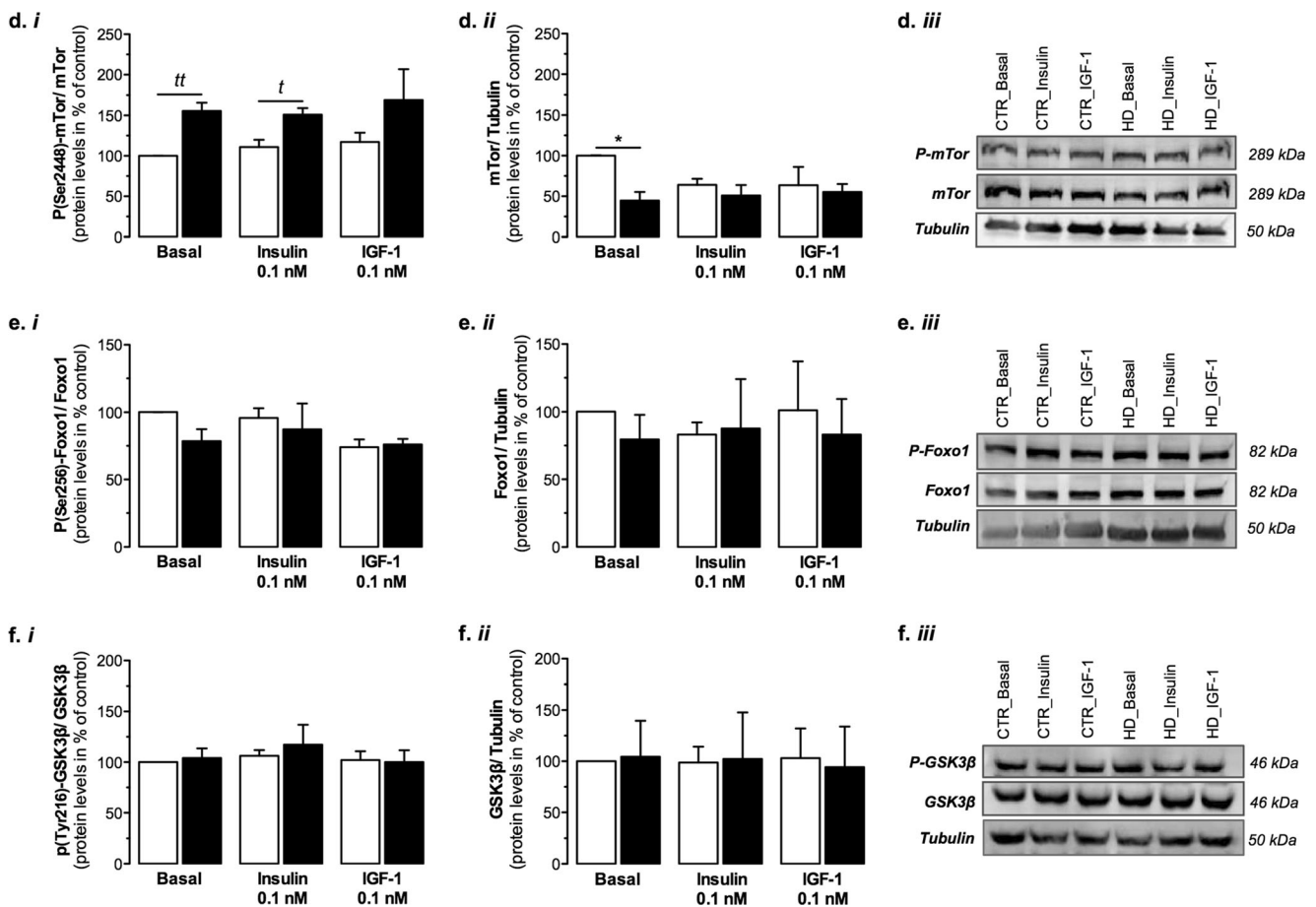


Fig. 1 (continued)

Indeed, their enzymatic activities can be negatively regulated by Akt-mediated phosphorylation at Ser9, and positively regulated by Tyr216 phosphorylation [47]; however, we also found no differences in the levels of P(Tyr216)-GSK-3β (Fig. 1f).

Insulin and IGF-1 Promote Huntingtin Phosphorylation

Specific neuroprotective effect of IGF-1/Akt in HD appears to be mediated by direct phosphorylation of Htt by Akt at Ser421, blocking mHtt-induced cell death and inhibiting intranuclear inclusion formation [21, 30]. Figure 2 shows that decreased P(Ser421)-Htt in HD lymphoblasts is completely rescued by insulin and IGF-1 (both at 0.1 nM) (Fig. 2a). Although there was a decrease in phosphorylation, Htt protein levels remained unchanged in HD and CTR cells (Fig. 2b) and upon exposure to insulin or IGF-1 (data not shown).

Insulin and IGF-1 Prevent Impairment of Energy Metabolism

We further analyzed the effect of insulin and IGF-1 on cellular adenine nucleotides, ATP, ADP, and AMP. HD lymphoblasts exhibited a decrease in ATP levels and an increase in ADP and AMP levels, compared to CTR lymphoblasts (Fig. 3a, i–iii).

Following incubation with 0.1 nM insulin or IGF-1, a significant increase in ATP levels was observed in HD lymphoblasts, which appeared to derive from ADP and AMP (Fig. 3a, i–iii). Concomitantly with ATP decrease, a significant decrease in phosphocreatine levels was observed in HD, compared to CTR lymphoblasts, which were completely recovered upon treatment with insulin or IGF-1 (Fig. 3b). Moreover, the amount of lactate was shown to be significantly higher in untreated HD cells, when compared to CTR cells (Fig. 3d); insulin or IGF-1 (0.1 nM) caused a decrease in lactate levels in HD lymphoblasts. The intracellular levels of lactate in CTR cells were not significantly affected in the presence of insulin or IGF-1. Although there were significant alterations in lactate levels in HD cells, no visible changes were observed in pyruvate levels (Fig. 3c).

IGF-1/P-Htt Pathway Recovers Mitochondrial Function in HD Lymphoblasts

There are several evidences that mitochondrial dysfunction plays a critical role in HD pathogenesis [7, 17, 18]. In order to evaluate whether mitochondrial dysfunction can be the source of lower ATP levels, we assessed O₂ consumption in HD and CTR lymphoblasts (Fig. 4a–c). Under basal conditions, HD

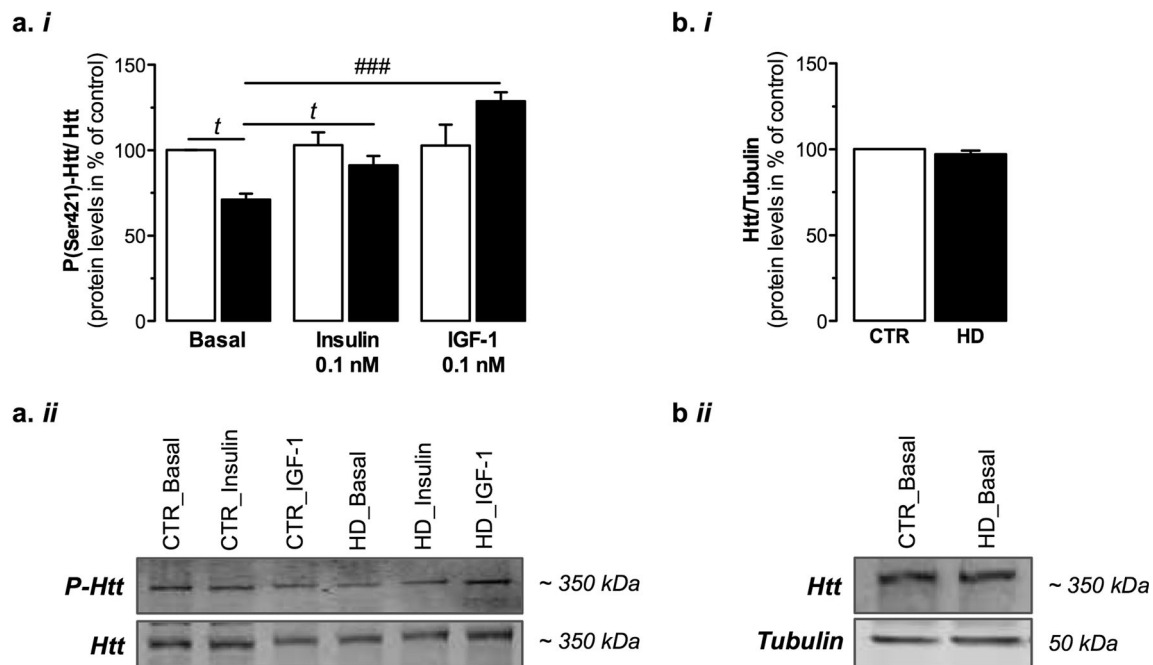


Fig. 2 IGF-1 and insulin promote huntingtin phosphorylation in HD lymphoblasts. CTR or HD lymphoblasts were untreated (basal) or treated with 0.1 nM insulin or IGF-1 in culture medium (RPMI-1640) for 24 h at 37°C. Levels of P(Ser421)Htt (**a**) and Htt (**b**) were analyzed by Western blotting. Data are the mean±SEM from four independent experiments,

expressed as percentage of CTR, considering **a** 2.08 ± 0.39 INT/mm² and **b** 27.17 ± 1.03 INT/mm² as 100 %. Statistical analysis: ^t $P < 0.05$ vs respective CTR (Student's *t* test); ^{###} $P < 0.001$ vs untreated HD (two-way ANOVA, followed by Bonferroni post hoc test)

lymphoblasts showed a lower rate of O₂ consumption compared to CTR lymphoblasts (Fig. 4a), suggesting decreased activity of mitochondrial respiratory chain, which was

prevented by pre-exposure to 0.1 nM IGF-1, but not by insulin (Fig. 4a). Maximal O₂ consumption, defined in the presence of CCCP (mitochondrial uncoupler) plus oligomycin (ATP

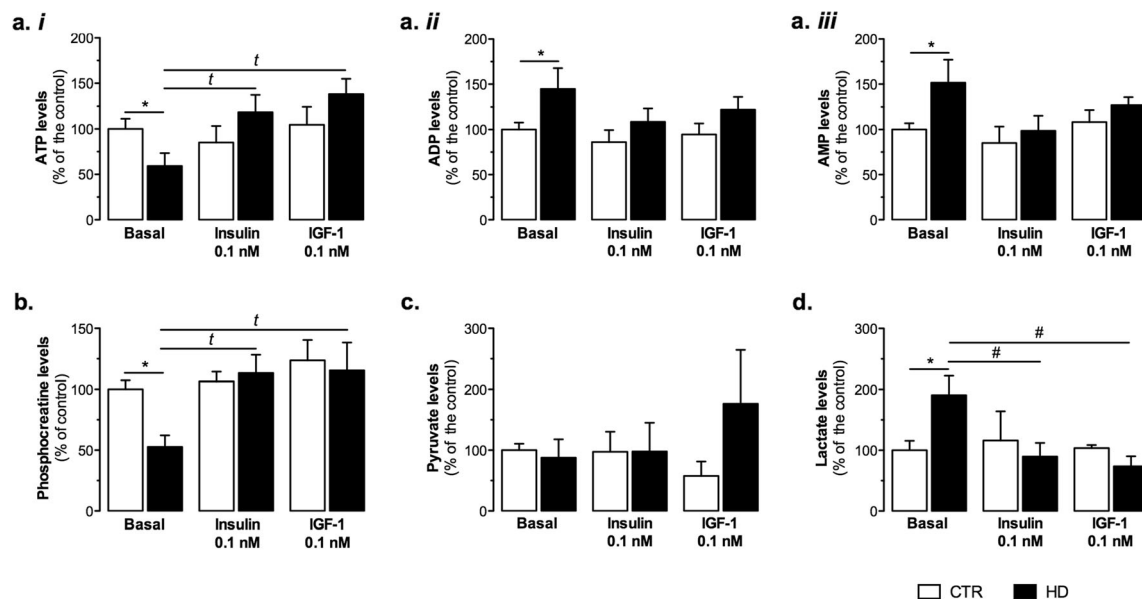


Fig. 3 IGF-1 and insulin rescued energy metabolism in HD lymphoblasts. CTR or HD lymphoblasts were untreated (basal) or treated with 0.1 nM insulin or IGF-1 in culture medium (RPMI-1640) for 24 h at 37°C. Energy metabolism was evaluated by determining levels of ATP (**a.i**), ADP (**a.ii**), AMP (**a.iii**), phosphocreatine (**b**), pyruvate (**c**), and lactate (**d**). Data are the mean±SEM from four independent experiments performed in duplicates, expressed as the % of CTR, considering **a** $1.3 \pm$

0.3 nmol/mg prot (**i**), 1.4 ± 0.2 pmol/mg prot (**ii**), 1.6 ± 0.3 pmol/mg prot (**iii**), **b** 67.23 ± 21.98 pmol/mg prot, **c** 17.01 ± 1.0 nmol/mg prot as 100 %, and **d** 0.27 ± 0.04 nmol/mg prot as 100 %. Statistical significance: ^t $P < 0.05$ vs untreated HD (Student's *t* test); ^{*} $P < 0.05$ vs CTR; [#] $P < 0.05$ vs untreated HD (two-way ANOVA, followed by Bonferroni post hoc test)

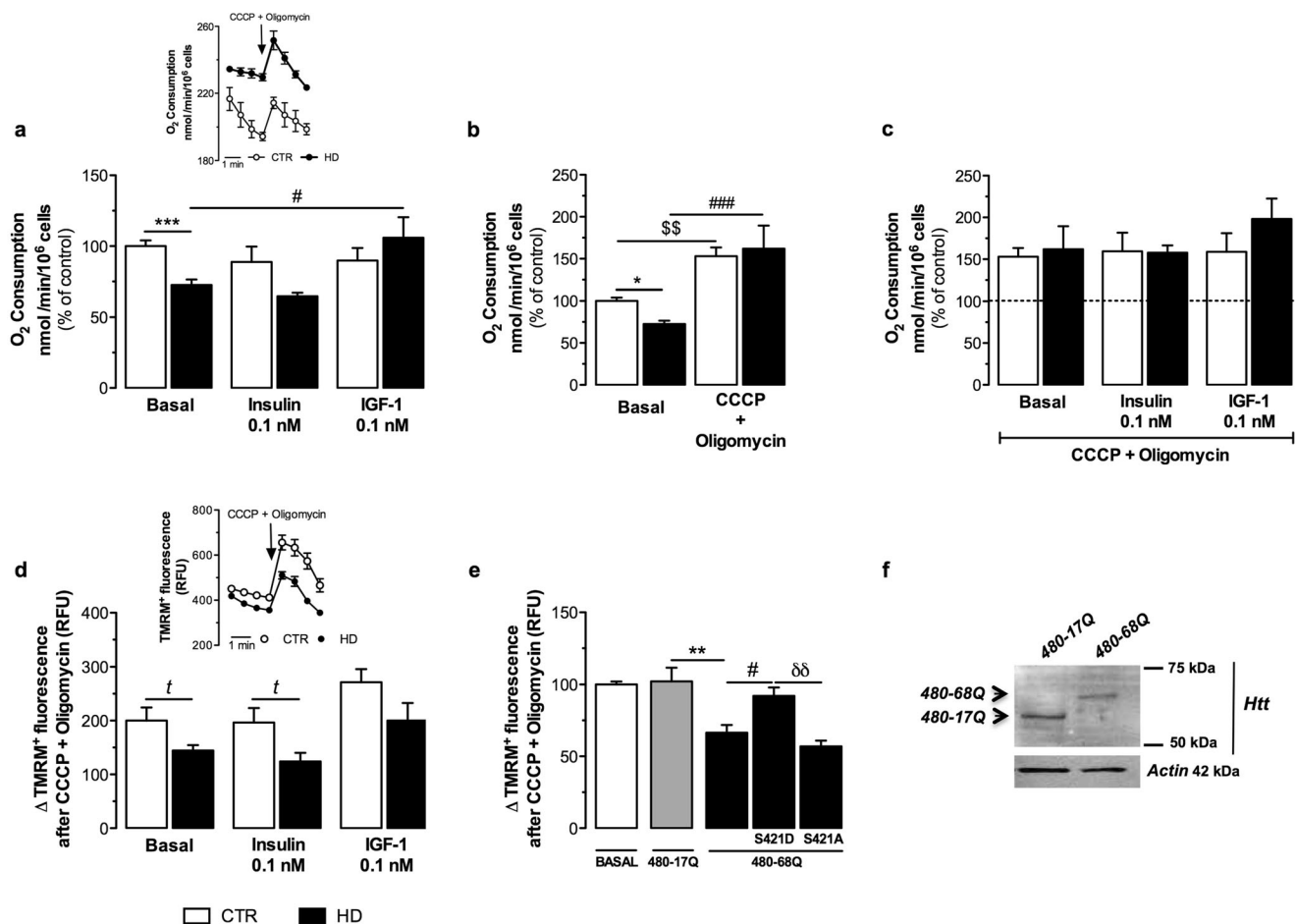


Fig. 4 IGF-1/P-Htt pathway ameliorates the rate of O_2 consumption and mitochondrial membrane potential in HD lymphoblasts. CTR or HD lymphoblasts were untreated (basal) or treated with 0.1 nM insulin or IGF-1 in culture medium (RPMI-1640) for 24 h at 37°C. Basal recording rate of O_2 consumption (**a**); maximum respiration was achieved after addition of CCCP plus oligomycin to untreated (**b**) or insulin and IGF-1 treated (**c**) CTR or HD lymphoblasts. TMRM⁺ fluorescence was recorded after complete mitochondrial membrane depolarization (**d**, **e**). CTR lymphoblasts were transfected with plasmid constructs (480-17Q, 480-68Q, 480-68-S421D, and 480-68-S421A) previously described by Humbert et al. [21] 48 h before the experiment (**e**). Results were expressed as the

synthase inhibitor), as defined in Fig. 4a (insert) and b, was largely the same in CTR or HD lymphoblasts, in the absence or presence of insulin or IGF-1 (Fig. 4c).

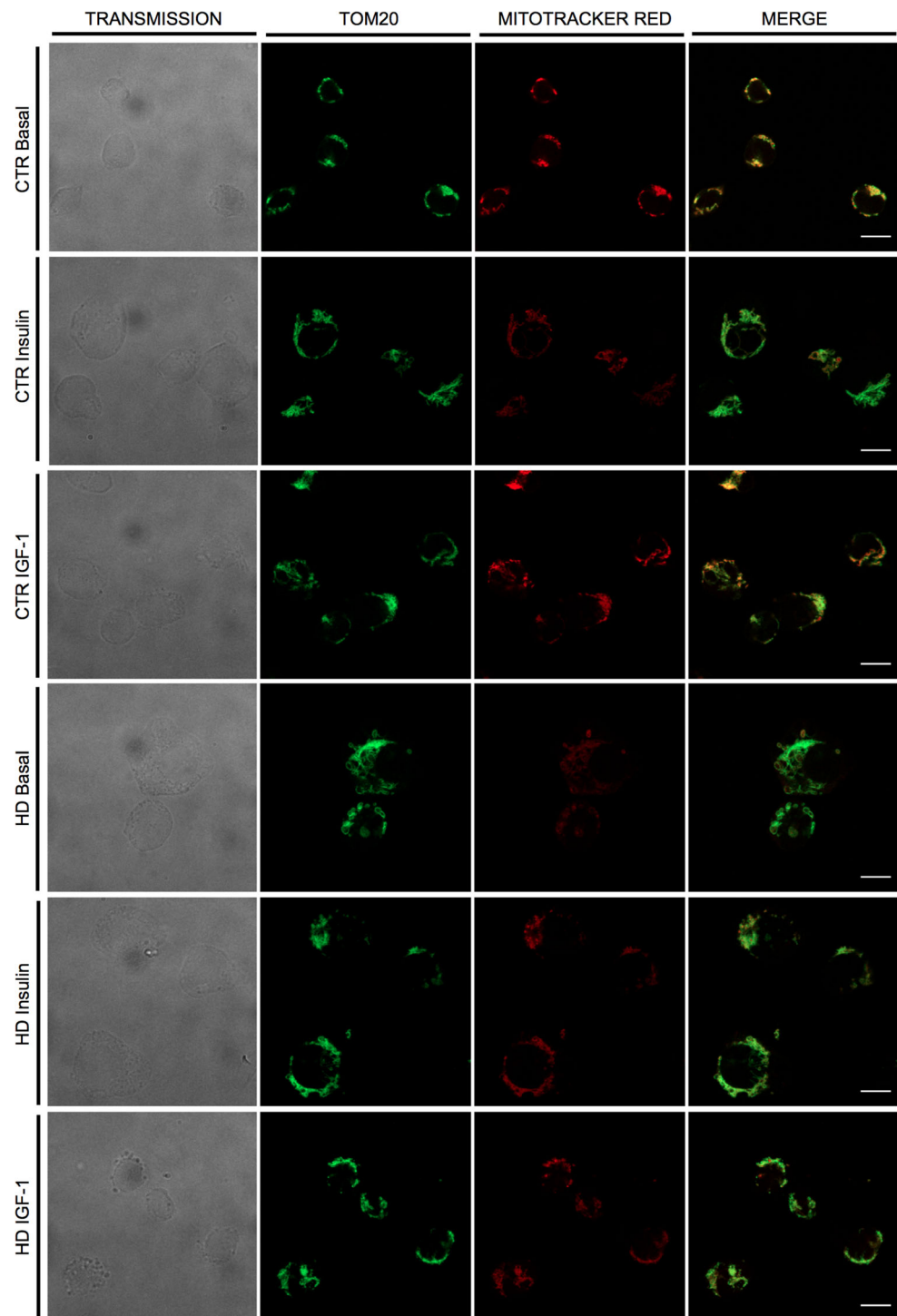
We further evaluated mitochondrial membrane potential ($\Delta\psi_m$) before and after complete mitochondrial depolarization with CCCP plus oligomycin (Fig. 4d, insert). HD lymphoblasts exhibited a lower mitochondrial retention of TMRM⁺, largely suggesting lower $\Delta\psi_m$, compared to CTR lymphoblasts; however, this decrease became insignificant in the presence of 0.1 nM IGF-1 (Fig. 4d), suggesting an amelioration of mitochondrial function, in accordance with the O_2 consumption (Fig. 4a). Under the same experimental conditions, insulin had no significant effects on $\Delta\psi_m$. These observations were further confirmed by qualitative fluorescence imaging with MtT Red (Fig. 5). MtT Red is an $\Delta\psi_m$ -sensitive

difference between the increase of TMRM⁺ fluorescence upon addition of CCCP plus oligomycin and basal fluorescence values. Inserts show representative traces of O_2 consumption (in **a**) or TMRM⁺ fluorescence (in **d**). The presence of truncated wild-type Htt (17 polyQ) or mHtt (68 polyQ) was detected by Western blotting (**f**). Data are the mean \pm SEM of three to four experiments performed in duplicates or triplicates. Statistical analysis: ^t $P < 0.05$ vs untreated HD (Student's *t* test); * $P < 0.05$, ** $P < 0.01$, *** $P < 0.001$, ^{\$\$} $P < 0.01$ vs untreated CTR; # $P < 0.05$, ### $P < 0.001$ vs untreated HD; ^{δδ} $P < 0.01$ vs S421D HD (two-way ANOVA, followed by Bonferroni post hoc test)

positively charged fluorescent probe that is rapidly taken up into the negatively charged mitochondria [48]. Our results show a decrease in MtT Red fluorescence in HD compared to CTR lymphoblasts (Fig. 5), thus reducing its colocalization with TOM20, a mitochondria marker that remains unchanged between genotypes (CTR vs HD) (Table 1). Moreover, IGF-1 treatment appears to effectively rescue the decrease in $\Delta\psi_m$ in HD cells, as observed by the increase in MtT Red fluorescence, in accordance with TMRM⁺ fluorescence data. Interestingly, insulin appears to have the same effect as IGF-1 (Fig. 5), although these results have not been confirmed with TMRM⁺.

Considering these results, we hypothesized that beneficial effect of IGF-1 on mitochondrial function might be related with Htt phosphorylation. Therefore, we transfected CTR

Fig. 5 IGF-1 and insulin rescue mitochondrial membrane potential in HD lymphoblasts. Representative confocal microscope images of CTR and HD lymphoblasts untreated (basal) or treated with 0.1 nM insulin or IGF-1 for 24 h, at 37°C. Lymphoblasts were stained with MitoTracker Red CMXRos (MtT Red, 500 nM) (red) and anti-TOM20 (green). *Left* Transmission image, *middle left* TOM20 signal, *middle right* MtT Red signal, *right* Merge image. Scale bar: 10 μ m



lymphoblasts with 480 amino acid-Htt fragments containing a stretch of 17 (480-17) or 68 (480-68) glutamines, being the efficiency of transfection confirmed by Western blotting (Fig. 4f). Moreover, two more constructs were transfected: one containing a serine to aspartate mutation at the 421 site, maintaining Htt constitutively phosphorylated (480-68-S421D) and another one containing a serine to alanine mutation, thus inhibiting Htt phosphorylation (480-68-S421A). In

accordance with data obtained in HD lymphoblasts, we observed a significant decrease in $\Delta\psi_m$ in lymphoblasts transfected with 480-68 construct, compared with 480-17 transfected lymphoblasts. Constitutive Htt phosphorylation (S421D) was able to fully restore $\Delta\psi_m$ in lymphoblasts carrying the mutant stretch; In contrast, serine to alanine mutation completely deregulated $\Delta\psi_m$ (Fig. 4e). These data largely suggested that amelioration of mitochondrial function

Table 1 Mitochondrial-relevant proteins in human HD and CTR lymphoblasts

Proteins of interest	CTR (mean±SEM) (<i>n</i>)	HD (mean±SEM) (<i>n</i>)
Mitochondrial-encoded ETC subunits		
Mitochondrial complex I (subunit, 20 kDa)/hsp60 (T)	100.0±16.65 (10)	73.24±19.56 (11)
Mitochondrial complex I (subunit, 20 kDa)/hsp60 (M)	100.0±25.20 (5)	93.72±17.06 (8)
Mitochondrial complex IV (subunit SI)/hsp60 (T)	100.0±13.35 (5)	87.73±12.55 (4)
Mitochondrial complex IV (subunit SI)/hsp60 (M)	100.0±13.10 (5)	103.66±12.61 (9)
Nuclear-encoded ETC subunits		
Mitochondrial complex I (subunit, 30 kDa)/hsp60 (T)	100.0±2.13 (6)	98.03±12.00 (8)
Mitochondrial complex II (subunit, 70 kDa)/hsp60 (T)	100.0±15.58 (9)	93.00±15.78 (11)
Mitochondrial translocases and chaperones		
Hsp60/tubulin (T)	100.0±3.14 (9)	112.9±9.22 (15)
TOM20/hsp60 (M)	100.0±0.11 (3)	97.39±36.98 (3)
TOM40/hsp60 (M)	100.0±1.58 (3)	99.16±17.86 (3)
Prohibitin (PHB)/hsp60 (M)	100.0±10.46 (5)	103.02±12.28 (9)
Transcription factors		
Mitochondrial transcription factor (Tfam)/hsp60 (M)	100.0±8.08 (9)	60.06±6.80 (8)**
p65/hsp60 (M)	100.0±12.78 (3)	95.79±8.06 (6)
p53/hsp60 (M)	100.0±13.19 (3)	94.39±15.96 (9)
Apoptotic proteins		
Bax/hsp60 (M)	100.0±3.48 (3)	90.14±27.42 (3)
Bax/tubulin (C)	100.0±5.85 (3)	92.68±10.47 (3)
AIF/tubulin (T)	100.0±9.161 (5)	82.74±6.74 (4)
Cytochrome c/hsp60 (M)	100.0±9.12 (6)	65.97±6.55 (4)*
Cytochrome c/tubulin (C)	100.0±6.29 (3)	68.52±14.47 (3)
Cytochrome c/tubulin (T)	100.0±0.00 (3)	70.30±0.78 (3)**

Relative changes in the levels of mitochondrial- and nuclear-encoded proteins from total (T), mitochondrial (M) and/or cytosolic (C)-enriched fractions from human HD or CTR lymphoblasts. Proteins of the mitochondria electron transport chain, mitochondrial translocases of the outer membrane, 20 and 40 subunits (TOM20 and TOM40, respectively) and the mitochondrial chaperones hsp60 and prohibitin (PHB), transcription factors, and apoptotic proteins. The results are the mean±SEM of the indicated number of experiments (in brackets) normalized to hsp60 or tubulin (as indicated) and are represented as the % of the CTR group

* $P < 0.05$; ** $P < 0.01$ vs CTR (by the Student's *t* test)

induced by IGF-1 in HD lymphoblasts occurs through phosphorylation of mHtt at Ser421.

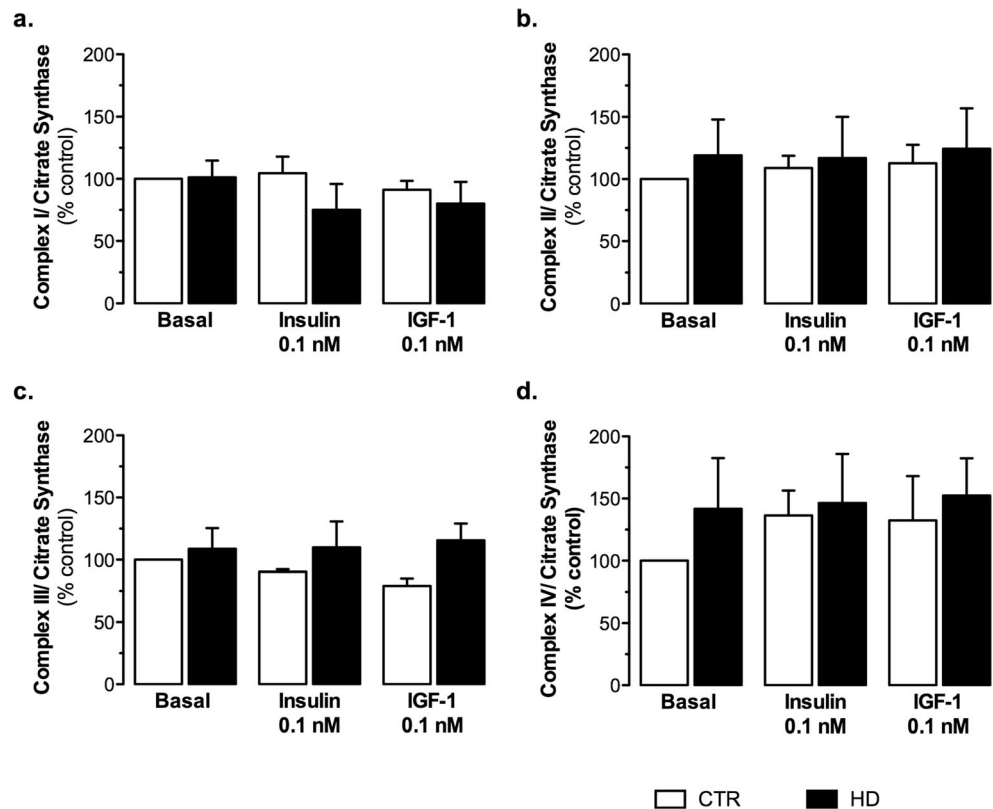
Unchanged Protein Expression or Activity of Mitochondrial Complexes, But Decreased Cytochrome c in HD Lymphoblast Mitochondria—Effect of Insulin and IGF-1

After observing the decrease in ATP production and oxygen consumption in HD lymphoblasts, we sought for changes in activity and expression of mitochondrial respiratory complexes and proteins. No significant differences in the activity of mitochondrial respiratory chain complexes I–IV were observed in HD versus CTR lymphoblasts (Fig. 6), corroborating previous data [11]. Table 1 shows that there are no statistical significant differences in protein levels of both mitochondrial- and nuclear-encoded subunits from electron transport chain (Table 1) either.

We also examined the relative changes in other mitochondrial proteins, including subunits of transporter outer membrane (TOM) complex, hsp60, and prohibitin, as well as mitochondrial transcription factors, namely, mitochondrial transcription factor A (Tfam), p65 and p53, but apart from Tfam, no statistical differences were found between HD and CTR cells (Table 1). Tfam is the major transcription factor of mitochondrial DNA (mtDNA) and also appears to protect mtDNA since it packages mtDNA into DNA–protein aggregates called mitochondrial nucleoids [49]. Tfam stimulates the transcription of the majority mitochondrial-encoded subunits [50]; nevertheless, complex I subunit of 20 kDa and complex IV subunit SI were not altered in HD lymphoblasts (Table 1). Despite this, we cannot exclude the hypothesis that this factor could be a key protein in mitochondrial dysfunction in this HD cell model.

Previous data in our lab showed mitochondrial-associated cell death in a peripheral model expressing mHtt, through the

Fig. 6 Mitochondrial respiratory chain specific activities of complexes I–IV are unchanged in HD lymphoblasts. CTR or HD lymphoblasts were untreated (basal) or treated with 0.1 nM insulin or IGF-1 in culture medium (RPMI-1640) for 24 h at 37°C. The activities of mitochondrial complexes I (a), II (b), III (c), and IV (d) were normalized to citrate synthase. Data are expressed as the mean \pm SEM from three to six independent experiments



activation of caspases, release of cytochrome c and AIF from mitochondria, and increased Bcl-2-associated X protein (Bax) levels [18]. Bearing this in mind, we also analyzed the levels of the apoptotic proteins Bax, AIF, and cytochrome c in HD lymphoblasts. A significant decline was detected in cytochrome c protein levels in mitochondria from HD lymphoblasts, which did not account for by an increase in the protein in the cytosol (Table 1), precluding any evidence for mitochondrial-driven apoptosis in these peripheral cells. Accordingly, cytochrome c total levels were significantly decreased in HD cells, largely suggesting that deficits in O_2 consumption can be due to decreased shuttling of electrons at cytochrome c level. Moreover, treatment with 0.1 nM IGF-1 rescued the decrease in cytochrome c in HD lymphoblasts (Fig. 7), revealing a protein modification at the electron transport chain that contributes for boosting mitochondrial function in the presence of this neurotrophic factor.

Altered Mitochondrial Ca^{2+} Accumulation in HD Lymphoblasts—Role of Insulin and IGF-1

Under the same experimental conditions, we measured the intracellular free levels of Ca^{2+} (Ca^{2+}_i) and the capacity of mitochondria to retain the ion. HD cells showed increased intracellular Ca^{2+} , which was exacerbated upon exposure to IGF-1 (Fig. 8a). Moreover, complete mitochondrial depolarization with CCCP plus oligomycin elicited a decrease in Ca^{2+}

release from mitochondria in HD lymphoblasts compared to CTR cells, highly suggestive of decreased mitochondria capacity to retain Ca^{2+} in HD lymphoblasts (Fig. 8b). However,

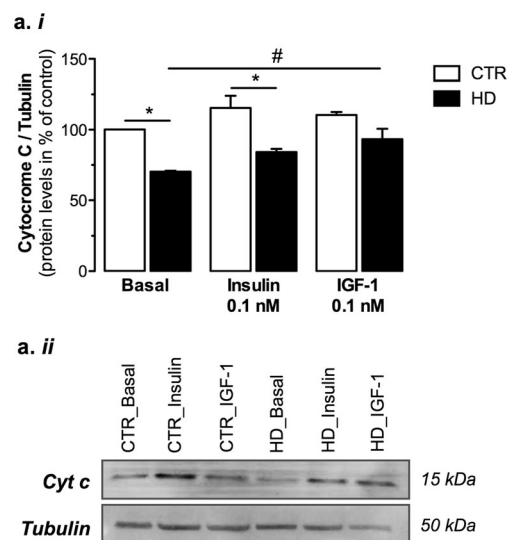
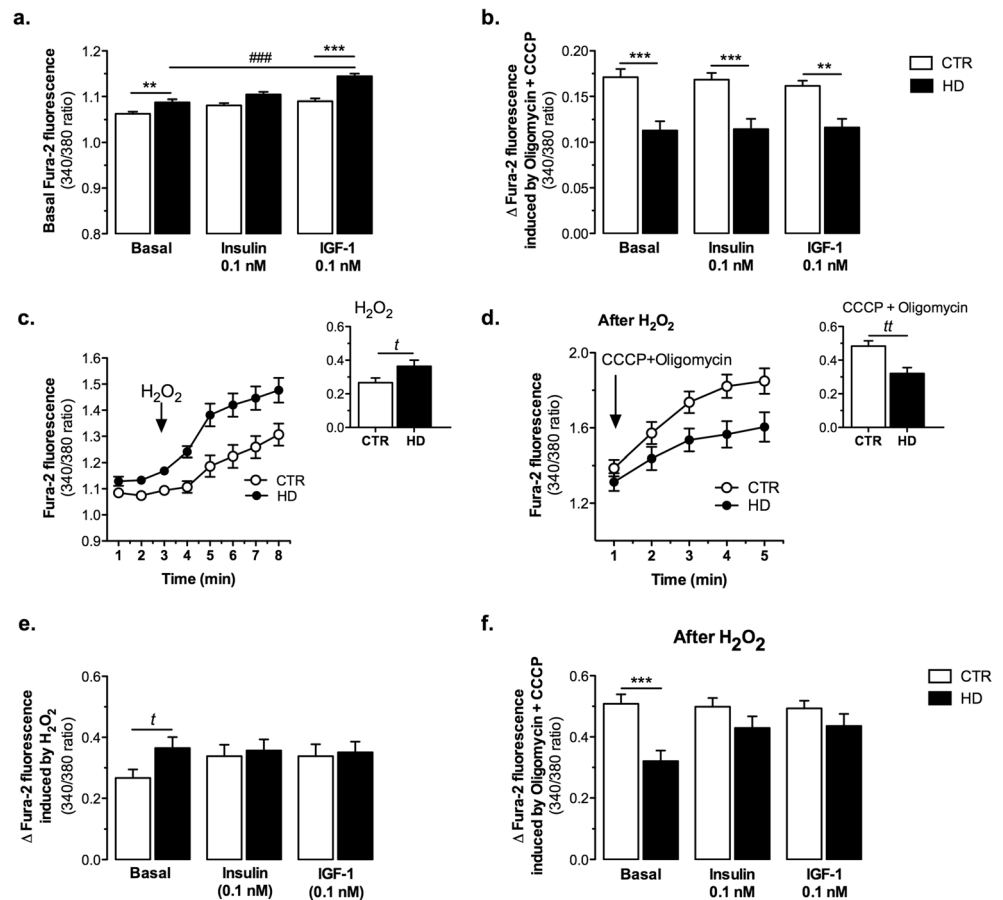


Fig. 7 IGF-1 enhances the levels of cytochrome c in HD lymphoblasts. CTR or HD lymphoblasts were untreated (basal) or treated with 0.1 nM insulin or IGF-1 in culture medium (RPMI-1640) for 24 h at 37°C. Total expression levels of cytochrome c were analyzed by Western blotting on 15 % SDS-PAGE and reprobed for tubulin (a i, ii). Data are the mean \pm SEM from three independent experiments, expressed as percentage of CTR, considering 0.48 ± 0.06 INT/mm² as 100 %. Statistical analysis: * $P < 0.05$ vs respective CTR; # $P < 0.05$ vs untreated HD (two-way ANOVA, followed by Bonferroni post hoc test)

Fig. 8 IGF-1 and insulin ameliorate mitochondrial Ca^{2+} accumulation in HD lymphoblasts subjected to H_2O_2 . CTR or HD lymphoblasts were untreated (basal) or treated with 0.1 nM insulin or IGF-1 in culture medium (RPMI-1640) for 24 h at 37°C . Basal intracellular Ca^{2+} levels (Ca^{2+}_i) levels were recorded in cells loaded with Fura-2/AM, without (a) or upon adding CCCP plus oligomycin (b) to completely depolarize the mitochondria in order to assess mitochondrial Ca^{2+} retention. Ca^{2+}_i were also recorded in untreated (c, d) or insulin/IGF-1-treated (e, f) lymphoblasts following stimulation with 1 mM H_2O_2 , in the absence (as in c) or presence (as in d) of CCCP plus oligomycin. Data are the mean \pm SEM of four independent experiments, performed in triplicates or quadruplicates. Statistical analysis: $^1P < 0.05$, $^uP < 0.05$ vs untreated CTR (Student's *t* test); $^{**}P < 0.01$, $^{***}P < 0.001$ vs respective CTR; $^{####}P < 0.001$ vs untreated HD lymphoblasts (two-way ANOVA, followed by Bonferroni post hoc test)



neither insulin nor IGF-1 augmented the mitochondrial capacity to accumulate Ca^{2+} .

We further analyzed the effect of adding H_2O_2 (1 mM) on Ca^{2+}_i levels. HD lymphoblasts exhibited an increase Ca^{2+}_i upon incubation with H_2O_2 , as compared to H_2O_2 -treated CTR lymphoblasts (Fig. 8c). In the presence of insulin or IGF-1, there were no significant changes between HD and CTR cells (Fig. 8e). Moreover, H_2O_2 -treated HD cells still showed decreased mitochondrial Ca^{2+} retention, examined after complete mitochondrial depolarization (Fig. 8d). This abnormal buffering capacity was partially but significantly restored following pre-exposure to both insulin and IGF-1 in H_2O_2 -treated HD lymphoblasts (Fig. 8f), suggesting protection by IGF-1 under conditions of oxidative stress.

Discussion

Recent evidences suggest that impaired metabolism plays an important role in the pathogenesis of HD-affected individuals, in both central and peripheral tissues [1, 8, 51], and the ability of insulin and IGF-1 to promote cell survival has been increasingly proven [22–24, 52] including in the context of HD [21, 30]. However, the neuroprotective role achieved by

insulin and IGF-1 has been questioned. Indeed, some studies showed that high levels of IGF-1 could increase mitochondrial and oxidative stress in HD mice [35] and cognitive decline in HD patients [33, 34]. Despite these observations, in the present work, we show that activation of IGF-1/insulin signaling pathway can rescue mitochondrial function and energy production in HD peripheral blood cells. In particular, we describe that IGF-1 ameliorates mitochondrial function (evidenced through increased O_2 consumption and $\Delta\psi_m$) in human HD lymphoblasts derived from HD patients, namely, through phosphorylation of Htt at Ser421 and increased levels of cytochrome c.

In previous studies, we showed that insulin, at micromolar concentrations, was able to activate both IR and IGF-1R in cortical neurons by stimulation of Tyr kinase activity [24]. In the present study, IGF-1 (at low nM) completely recovered IR, IGF-1R activation in HD lymphoblasts to levels observed in CTR cells, whereas insulin was less efficient when compared to IGF-1. Decreased IR, IGF-1R phosphorylation, due to the expression of mHtt, has been linked to decreased activation of ERK and Akt downstream signaling pathways, as observed in HD patients and mouse models expressing mHtt [21, 43, 53]. Concordantly, increased IGF-1 and IGF-1R expression was recently associated to enhanced ERK and

Akt phosphorylation [28]. The present work demonstrates that exposure to IGF-1 recovered Akt activation and increased P(Ser421)Htt levels; this is in accordance with our previous and more recent studies showing that neuroprotective effects mediated by IGF-1 require phosphorylation of Htt at Ser421 exerted by Akt, thus increasing neuronal survival and improving motor performance in HD YAC128 mice [21, 30]. Indeed, several phosphorylated sites have been identified on Htt protein; most of them were reported to be protective. Accordingly, phosphorylation at Ser241 by Akt restores Htt function in anterograde and retrograde axonal transport [54] and reduces the nuclear accumulation and cleavage of Htt [55]. Moreover, enhanced P(S421)Htt provided neuroprotection from *N*-methyl-D-aspartate-mediated excitotoxicity in YAC128 mouse model [56]. These evidences could be explained since serine residues phosphorylation in Htt N-terminal can suppress Htt accumulation by altering protein aggregation properties, thereby reducing toxicity [57–59].

Increased ERK phosphorylation was also shown to provide a pro-survival effect, a result already demonstrated before [28]. Surprisingly, the present work demonstrates that mTor activation, known to be involved in macroautophagy inhibition [60], appears to be increased in HD lymphoblasts when compared to CTR cells, despite presenting decreased total protein levels, which suggests a downregulation of autophagic mechanisms in HD cells. Indeed, increased levels of Ca^{2+} under basal conditions in HD lymphoblasts were previously reported to trigger mTor complex [61]. Moreover, apart from Akt, S6 kinase 1, a serine/threonine kinase directly activated by the ERK pathway, may be responsible for mTor activation [62, 63].

Previous studies performed by Seong et al. [64] demonstrated decreased ATP levels in lymphoblastoid cell lines obtained from homozygous HD patients, with 41–50 CAG repeats. Accordingly, our data also show decreased ATP levels in HD lymphoblasts, which were restored by IGF-1 and insulin. Other studies in muscle from HD patients and mHtt-transfected HeLa cells also showed a significant reduction in both ATP [65] and phosphocreatine [66] levels. In the present work, treatment of HD lymphoblasts with insulin or IGF-1 (at low nM) restored phosphocreatine levels, indicating that activation of insulin/IGF-1 signaling pathways can rescue energy levels in human blood cells expressing mHtt. Previously, we observed that insulin (at μ M range) completely prevented the decrease in intracellular ATP levels evoked by oxidative stress in primary cortical neurons [23].

Besides energetic defects, mitochondrial deregulation plays an important role in HD pathogenesis [7, 9, 18]. In fact, expression of mHtt caused loss of mitochondrial function [67] and altered mitochondrial morphogenesis with increased mitochondrial fission and reduced fusion [7]. In the present work, impaired mitochondrial function in HD lymphoblasts was confirmed by decreased O_2 consumption and reduced

$\Delta\psi_m$, as well as increased lactate levels, which may account for by a compensatory glycolytic response [68], as previously reported in the striatum and occipital cortex of HD patients [15, 69]. Similar increased glycolytic metabolism linked to moderate mitochondrial dysfunction was recently described by us in HD cybrid lines [19]. Although some studies advocated increased oxygen consumption, while others showed no alterations [70, 71], striatal *STHdh*^{Q111} cell lines evidenced decreased O_2 consumption and ATP production [72]. In accordance, studies in yeast expressing a 103Q-Htt exhibited a significant decrease in O_2 consumption associated with dysfunctional mitochondrial respiratory chain complexes II and III activities [73]. Recently, we also showed reduced activity of complex I in human platelets derived from pre-symptomatic and symptomatic HD carriers, evidencing mitochondrial changes before the onset of HD clinical symptoms [12]. Unlike these evidences, HD lymphoblasts [11] and cybrids [18] showed no changes in the activity of mitochondrial complexes I–IV or in the protein levels of complex subunits [74]. Indeed, our study also shows unchanged mitochondrial complexes activity and unaltered levels of the mitochondrial respiratory chain subunit proteins; despite this, we observed decreased levels of cytochrome c in HD lymphoblast's mitochondria. This observation and the fact that this protein uses the heme group as a redox intermediate for the electron transfer between complexes III and IV [75] may explain decreased O_2 consumption without changes in mitochondrial complexes expression and activity in HD lymphoblasts. Accordingly, cytochrome c mouse fibroblasts mutants were not able to assemble or stabilize cytochrome c oxidase (complex IV), causing respiratory deficits in the cell [76]. The loss of $\Delta\psi_m$ in HD lymphoblasts, observed in our study, could be related to disrupted proton translocation, as a consequence of decreased cytochrome c, due to the an interaction of mHtt with the outer mitochondrial membrane [17, 67]. Moreover, decreased Tfam levels can also contribute for this dysfunction; apart from being a relevant mitochondrial transcriptional factor, Tfam has multiple roles in the maintenance of mtDNA [77]. Indeed, we previously confirmed the presence of different patterns of mtDNA variations in human HD cybrids, despite the lack of differences in mitochondrial complexes activities [18].

Importantly, the role of phosphorylated Htt at Ser421, previously described to be triggered by the IGF-1/Akt pathway [21], was further demonstrated to rescue mitochondrial function in lymphoblasts expressing constitutively phosphorylated Htt with 68 polyQ (480-68-S421D); under these conditions, $\Delta\psi_m$ was completely restored to the levels of lymphoblasts expressing 17 polyQ. This effect seems to be specific since inhibition of Htt phosphorylation, following expression of 480-68-S421A, precluded $\Delta\psi_m$ recovering. Indeed, we previously showed that activation of IGF-1/Akt pathway was able to inhibit neuronal death induced by mHtt

[21] and ameliorated brain energy metabolism in YAC128 mice [30]. The present work further suggests that neuroprotection achieved by insulin and IGF-1 may be due to an improvement of mitochondrial function and consequent rectified cellular energy levels. Of relevance, decreased cytochrome c levels were largely recovered by IGF-1 only, supporting increased mitochondrial function through normalization of O_2 consumption and $\Delta\psi_m$.

Bioenergetics is not the only role played by mitochondria, as the organelle is also a key mediator of apoptosis and can be linked, directly and/or indirectly, to many common deleterious processes involved in neurodegeneration. Previous studies in neuronal cells expressing N-terminal mHtt revealed activation of caspase-3 with no significant release of apoptotic proteins, namely, cytochrome c and AIF into the cytosol [78]. However,

HD cybrids showed increased cytochrome c and AIF release from mitochondria, associated with the translocation of pro-apoptotic protein Bax to mitochondria [18]. Bax overexpression was also shown to be present in B lymphocytes obtained from human patients and associated with decreased $\Delta\psi_m$ [9]. Furthermore, we showed recently the release of cytochrome c and AIF and caspase-3 activation in HD knock-in striatal cells [79]. Nevertheless, human HD lymphoblasts used in the present study did not exhibit activation of intrinsic apoptotic pathway under basal conditions. However, calcium homeostasis appears to be deregulated in these cells; in fact, decreased $\Delta\psi_m$ and increased susceptibility to Ca^{2+} loads are other consequences of mitochondrial dysfunction, directly correlated with CAG repeat expansion, as shown previously [80, 81]. In the present study, impaired calcium homeostasis in HD human cells was evidenced through Ca^{2+}_i rise under basal

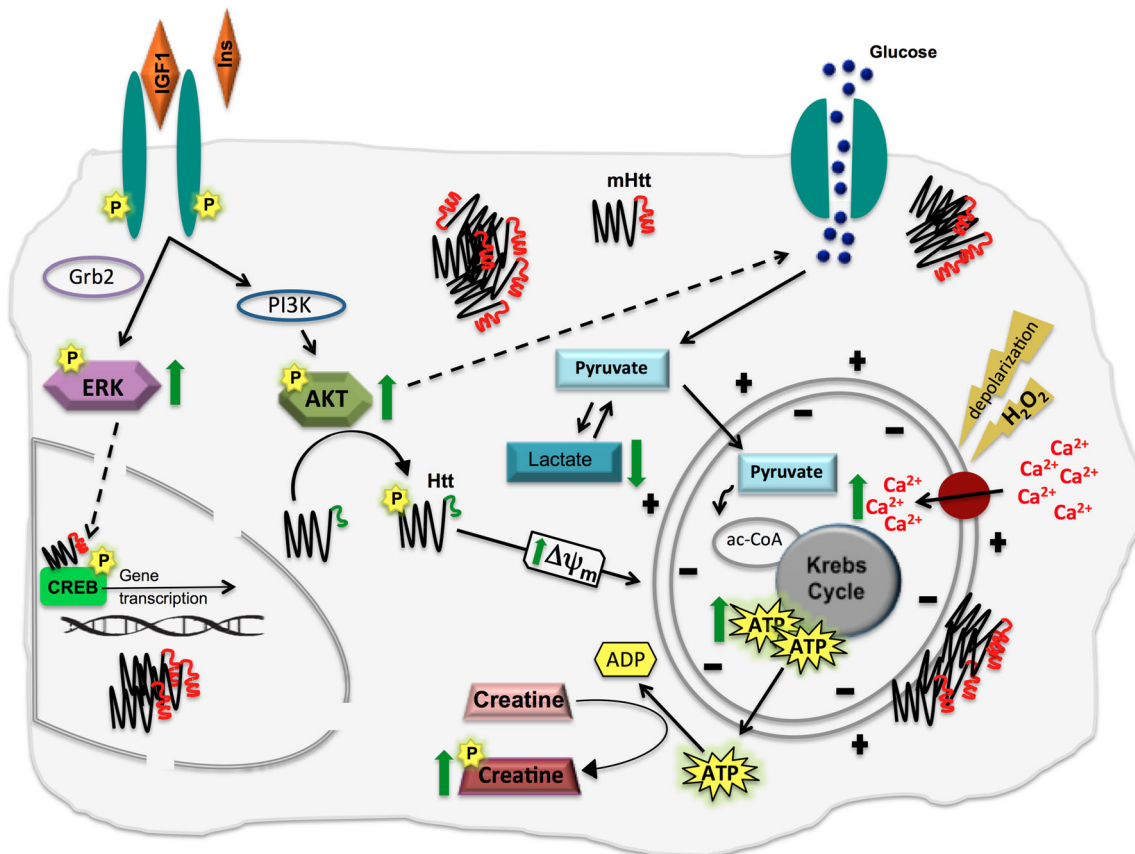


Fig. 9 IGF-1/Akt/P-Htt signaling pathway promotes protection against mHtt-mediated mitochondrial and metabolic dysfunction in HD lymphoblasts. Treatment with insulin or IGF-1 lead to multiple changes (represented in *green arrows*) through the phosphorylation of IR and/or IGF-1R, further leading to the activation of PI-3K/Akt and ERK signaling pathways. Active Akt directly phosphorylates Htt at Ser421, which in turn can rescue the $\Delta\psi_m$ in HD lymphoblasts. Moreover, activated ERK can translocate to the nucleus and phosphorylate transcription factors (such as CREB, among others), which in turn can bind promoters of many genes important in promoting growth and preventing apoptosis (e.g., [84]). Under oxidative stress (evoked by H_2O_2), Ca^{2+}_i levels are

increased, along with decreased mitochondrial Ca^{2+} accumulation, being the later recovered by IGF-1 and insulin. At metabolic level, insulin and particularly IGF-1 are able to rescue cellular energy status by increasing ATP and phosphocreatine levels and decreasing lactate levels. *PI-3K* Phosphatidylinositol 3-kinase, *Grb2* growth factor receptor-bound protein, *Akt* protein kinase B, *ERK* extracellular signal regulated kinase, *Htt* huntingtin, *mHtt* mutant huntingtin, $\Delta\psi_m$ mitochondrial membrane potential, *CREB* cAMP response element-binding protein, H_2O_2 hydrogen peroxide, *ac-CoA* acetyl-coenzyme A, *P* phosphorylation, *Ins* insulin, *IGF1* insulin growth factor 1

conditions and following exposure to H_2O_2 , suggesting a deficiency in the mechanisms that underlie the regulation of Ca^{2+}_i , in agreement with previous publications [67, 72]. Accordingly, HD lymphoblasts mitochondria also exhibited reduced capacity to take up Ca^{2+} , as observed following decreased release of Ca^{2+} into the cytosol of HD lymphoblasts after complete mitochondrial depolarization. Our results also evidenced that IGF-1 increased basal Ca^{2+}_i levels. Indeed, IGF-1 was previously shown to induce an increase in cytosolic Ca^{2+} mediated by phospholipase C gamma (PLC γ)/inositol 1,4,5-triphosphate (IP $_3$)-dependent signaling pathways in peripheral cells [82, 83], which may justify the observed increase in intracellular Ca^{2+} in HD lymphoblasts. Interestingly, in H_2O_2 pre-treated HD cells, IGF-1 and insulin improved mitochondrial Ca^{2+} uptake capacity, again pointing out the protective function of these peptides under oxidative stress conditions. Data suggest that increased Htt phosphorylation evoked by IGF-1/insulin may exert a protective role in stress-induced mitochondrial Ca^{2+} defects. In addition, in our lab, insulin and IGF-1 (also at low nM) improved mitochondrial function and reduced mitochondrial-driven reactive oxygen species caused by mHtt in HD knock-in striatal cells (Ribeiro and co-authors, unpublished data).

Altogether, our findings present strong evidence that mHtt-mediated disruption of insulin/IGF-1 downstream pathways, including Htt phosphorylation at Ser421, can lead to mitochondrial and metabolic dysfunction in HD human peripheral blood cells, namely, lymphoblastoid cell lines. Exposure to IGF-1 (in particular) and insulin play an important role in rescuing features of mitochondrial abnormalities and energy deficits, namely, by increasing $\Delta\psi_m$, cytochrome c protein levels and restoring mitochondrial Ca^{2+} uptake capacity upon an oxidant stress stimulus (Fig. 9). More specifically, we demonstrate that IGF-1 enhances mitochondrial function in human HD peripheral cells through increased activation of intracellular signaling pathways and Htt phosphorylation at Ser421.

Acknowledgments We wish to thank Doctor Luísa Cortes, head of Microscope Imaging Center of Coimbra (MICC) of CNC for the confocal image acquisition and analysis. This work was supported by “Fundação para a Ciência e Tecnologia” (FCT), Portugal, grants reference PTDC/SAU-FCF/66421/2006 and PTDC/SAU-FCF/108056/2008, and co-financed by COMPETE-“Programa Operacional Factores de Competitividade,” QREN, and the European Union (FEDER-“Fundo Europeu de Desenvolvimento Regional”). CNC is supported by project PEst-C/SAU/LA0001/2013-2014. L. Naia, M. Ribeiro, and M.J. Ribeiro are supported by Ph.D. fellowships from FCT (SFRH/BD/86655/2012, SFRH/BD/88983/2012, and SFRH/BD/41285/899/2007, respectively). T. Cunha-Oliveira, A.I. Duarte, T.R. Rosenstock, and M.N. Laço are supported by postdoctoral fellowships from FCT (SFRH/BPD/34711/2007, SFRH/BPD/26872/2006, SFRH/BPD/44246/2008, and SFRH/BPD/91811/2012, respectively).

Conflicts of Interest Statement The authors declare that they have no conflicts of interest.

References

- Gil JM, Rego AC (2008) Mechanisms of neurodegeneration in Huntington's disease. *Eur J Neurosci* 27:2803–2820
- Zuccato C, Valenza M, Cattaneo E (2009) Molecular mechanisms and potential therapeutic targets in Huntington's disease. *Physiol Rev* 90:905–981
- MacDonald ME, Gines S, Gusella JF, Wheeler VC (2003) Huntington's disease. *NeuroMolecular Med* 4:7–20
- Vonsattel JP, DiFiglia M (1998) Huntington disease. *J Neuropathol Exp Neurol* 57:369–384
- Cattaneo E, Rigamonti D, Goffredo D, Zuccato C, Squitieri F, Sipione S (2001) Loss of normal huntingtin function: new developments in Huntington's disease research. *Trends Neurosci* 24:182–188
- Ribeiro M, Rosenstock TR, Cunha-Oliveira T, Ferreira IL, Oliveira CR, Rego AC (2012) Glutathione redox cycle dysregulation in Huntington's disease knock-in striatal cells. *Free Radic Biol Med* 53:1857–1867
- Kim J, Moody JP, Edgerly CK, Bordiuk OL, Cormier K, Smith K, Beal MF, Ferrante RJ (2010) Mitochondrial loss, dysfunction and altered dynamics in Huntington's disease. *Hum Mol Genet* 19:3919–3935
- Rosenstock TR, Duarte AI, Rego AC (2010) Mitochondrial-Associated Metabolic Changes and Neurodegeneration in Huntington's disease—from Clinical Features to the Bench. *Curr Drug Targets* 11:1–16
- Almeida S, Sarmiento-Ribeiro AB, Januário C, Rego AC, Oliveira CR (2008) Evidence of apoptosis and mitochondrial abnormalities in peripheral blood cells of Huntington's disease patients. *Biochem Biophys Res Commun* 374:599–603
- Pettegrew JW, Nichols JS, Stewart RM (1980) Membrane studies in Huntington's disease: steady-state fluorescence studies of intact erythrocytes. *Ann Neurol* 8:381–386
- Sawa A, Wiegand GW, Cooper J, Margolis RL, Sharp AH, Lawler JF Jr, Greenamyre JT, Snyder SH, Ross CA (1999) Increased apoptosis of Huntington disease lymphoblasts associated with repeat length-dependent mitochondrial depolarization. *Nat Med* 5:1194–1198
- Silva AC, Almeida S, Laço M, Duarte AI, Domingues J, Oliveira CR, Januário C, Rego AC (2013) Mitochondrial respiratory chain complex activity and bioenergetics alterations in human platelets derived from pre-symptomatic and symptomatic Huntington's disease carriers. *Mitochondrion* 13:801–809
- Sassone J, Colciago C, Cislighi G, Silani V, Ciammola A (2009) Huntington's disease: the current state of research with peripheral tissues. *Exp Neurol* 219:385–397
- Gu M, Gash MT, Mann VM, Javoy-Agid F, Cooper JM, Schapira AH (1996) Mitochondrial defect in Huntington's disease caudate nucleus. *Ann Neurol* 39:385–389
- Jenkins BG, Koroshetz WJ, Beal MF, Rosen BR (1993) Evidence for impairment of energy metabolism in vivo in Huntington's disease using localized 1H NMR spectroscopy. *Neurology* 43:2689–2695
- Lodi R, Schapira AH, Manners D, Styles P, Wood NW, Taylor DJ, Warner TT (2000) Abnormal in vivo skeletal muscle energy metabolism in Huntington's disease and dentatorubropallidolusian atrophy. *Ann Neurol* 48:72–76
- Song W, Chen J, Petrilli A et al (2011) Mutant huntingtin binds the mitochondrial fission GTPase dynamin-related protein-1 and increases its enzymatic activity. *Nat Med* 17:377–382
- Ferreira IL, Nascimento MV, Ribeiro M, Almeida S, Cardoso SM, Grazina M, Pratas J, Santos MJ, Januário C, Oliveira CR, Rego AC (2010) Mitochondrial-dependent apoptosis in Huntington's disease human cybrids. *Exp Neurol* 222:243–255
- Ferreira IL, Cunha-Oliveira T, Nascimento MV, Ribeiro M, Proença MT, Januário C, Oliveira CR, Rego AC (2011) Bioenergetics

- dysfunction in Huntington's disease human cybrids. *Exp Neurol* 231:127–134
20. Cole GM, Frautschy SA (2007) The role of insulin and neurotrophic factor signaling in brain aging and Alzheimer's disease. *Exp Gerontol* 42:10–21
 21. Humbert S, Bryson EA, Cordelieres FP, Connors NC, Datta SR, Finkbeiner S, Greenberg ME, Saudou F (2002) The IGF-1/Akt pathway is neuroprotective in Huntington's disease and involves Huntingtin phosphorylation by Akt. *Dev Cell* 2:831–837
 22. Duarte AI, Santos MS, Oliveira CR, Rego AC (2005) Insulin neuroprotection against oxidative stress in cortical neurons—involvement of uric acid and glutathione antioxidant defences. *Free Radic Biol Med* 39:876–889
 23. Duarte AI, Proenca T, Oliveira CR, Santos MS, Rego AC (2006) Insulin restores metabolic function in cultured cortical neurons subjected to oxidative stress. *Diabetes* 55:2863–2870
 24. Duarte AI, Santos P, Oliveira CR, Santos MS, Rego AC (2008) Insulin neuroprotection against oxidative stress is mediated by Akt and GSK-3 β signaling pathways and changes in protein expression. *Biochim Biophys Acta* 1783:994–1002
 25. Zheng WH, Kar S, Quirion R (2002) Insulin-like growth factor-1-induced phosphorylation of transcription factor FKHRL1 is mediated by phosphatidylinositol 3-kinase/Akt kinase and role of this pathway in insulin-like growth factor-1-induced survival of cultured hippocampal neurons. *Mol Pharmacol* 62:225–233
 26. Aberg MA, Aberg ND, Hedbäcker H, Oscarsson J, Eriksson PS (2000) Peripheral infusion of IGF-I selectively induces neurogenesis in the adult rat hippocampus. *J Neurosci* 20:2896–2903
 27. Trejo JL, Carro E, Torres-Aleman I (2001) Circulating insulin-like growth factor I mediates exercise-induced increases in the number of new neurons in the adult hippocampus. *J Neurosci* 21:1628–1634
 28. Sasone L, Reali V, Pellegrini L, Villanova L, Avenaggiato M, Marfe G, Rosa R, Nebbioso M, Tafani M, Fini M, Russo MA, Pucci B (2013) SIRT1 silencing confers neuroprotection through IGF-1 pathway activation. *J Cell Physiol* 228:1754–1761
 29. Chang HC, Yang YR, Wang PS, Kuo CH, Wang RY (2013) The neuroprotective effects of intramuscular insulin-like growth factor-I treatment in brain ischemic rats. *PLoS One* 8:e64015
 30. Lopes C, Ribeiro M, Duarte AI, Humbert S, Saudou F, Pereira de Almeida L, Hayden M, Rego AC (2014) IGF-1 intranasal administration rescues Huntington's disease phenotypes in YAC128 mice. *Mol Neurobiol* 49:1126–1142
 31. Pouladi MA, Xie Y, Skotte NH et al (2010) Full-length huntingtin levels modulate body weight by influencing insulin-like growth factor I expression. *Hum Mol Genet* 19:1528–1538
 32. Dalrymple A, Wild EJ, Joubert R et al (2007) Proteomic profiling of plasma in Huntington's disease reveals neuroinflammatory activation and biomarker candidates. *J Proteome Res* 6:2833–2840
 33. Saleh N, Moutereau S, Durr A, Krystkowiak P, Azulay JP, Tranchant C, Broussolle E, Morin F, Bachoud-Lévi AC, Maison P (2009) Neuroendocrine disturbances in Huntington's disease. *PLoS One* 4:e4962
 34. Saleh N, Moutereau S, Azulay JP, Verny C, Simonin C, Tranchant C, El Hawajri N, Bachoud-Lévi AC, Maison P (2010) High insulinlike growth factor I is associated with cognitive decline in Huntington disease. *Neurology* 75:57–63
 35. Sadagursky M, Cheng Z, Rozzo A, Palazzolo I, Kelley GR, Dong X, Kraic D, White MF (2011) IRS2 increases mitochondrial dysfunction and oxidative stress in a mouse model of Huntington disease. *J Clin Invest* 121:4070–4081
 36. Almeida S, Domingues A, Rodrigues L, Oliveira CR, Rego AC (2004) FK506 prevents mitochondrial-dependent apoptotic cell death induced by 3-nitropropionic acid in rat primary cortical cultures. *Neurobiol Dis* 17:435–444
 37. Stocchi V, Cucchiari L, Magnani M, Chiarantini L, Palma P, Crescentini G (1985) Simultaneous extraction and reverse-phase high-performance liquid chromatographic determination of adenine and pyridine nucleotides in human red blood cells. *Anal Biochem* 146:118–124
 38. Lamprecht W, Stein P, Heinz F, Weissner H (1974) Creatine phosphate. In: Bergmeyer H (ed) *Methods of enzymatic analysis*, vol 4. Academic Press, New York, pp 1777–1781
 39. Ragan CI, Wilson MT, Darley-Usmar VM, Lowe PN (1967) Subfractionation of mitochondria and isolation of the proteins of oxidative phosphorylation. In: Darley-Usmar VM, Rickwood D, Wilson MT (eds) *Mitochondria, a practical approach*. IRL Press, London, pp 79–112
 40. Hatefi Y, Stiggall DL (1978) Preparation and properties of succinate: ubiquinone oxidoreductase (complex II). *Methods Enzymol* 53:21–27
 41. Wharton DC, Tzagotoff A (1967) Cytochrome oxidase from beef heart mitochondria. *Methods Enzymol* 10:245–250
 42. Coore HG, Denton RM, Martin BR, Randle PJ (1971) Regulation of adipose tissue pyruvate dehydrogenase by insulin and others hormones. *Biochem J* 125:115–127
 43. Colin E, Régulier E, Perrin V, Dürr A, Brice A, Aebischer P, Deégion N, Humbert S, Saudou F (2005) Akt is altered in an animal model of Huntington's disease and in patients. *Eur J Neurosci* 21:1478–1488
 44. Stamper BD, Mecham B, Park SS, Wilkerson H, Farin FM, Bever RP, Bammler TK, Mangravite LM, Cunningham ML (2012) Transcriptome correlation analysis identifies two unique craniosynostosis subtypes associated with IRS1 activation. *Physiol Genomics* 44:1154–1163
 45. Rechler MM, Zapf J, Nissley SP, Froesch ER, Moses AC, Podskalny JM, Schilling EE, Humbel RE (1980) Interactions of insulin-like growth factors I and II and multiplication-stimulating activity with receptors and serum carrier proteins. *Endocrinology* 107:1451–1459
 46. Summers SA, Kao AW, Kohn AD, Backus GS, Roth RA, Pessin JE, Birnbaum MJ (1999) The role of glycogen synthase kinase 3 β in insulin-stimulated glucose metabolism. *J Biol Chem* 274:17934–17940
 47. Cole A, Frame S, Cohen P (2004) Further evidence that the tyrosine phosphorylation of glycogen synthase kinase-3 (GSK3) in mammalian cells is an autophosphorylation event. *Biochem J* 377:249–255
 48. Macho A, Decaudin D, Castedo M, Hirsch T, Susin SA, Zamzami N, Kroemer G (1996) Chloromethyl-X-Rosamine is an aldehyde-fixable potential-sensitive fluorochrome for the detection of early apoptosis. *Cytometry* 25:333–340
 49. Kaufman BA, Durisic N, Mativetsky JM, Costantino S, Hancock MA, Grutter P, Shoubbridge EA (2007) The mitochondrial transcription factor TFAM coordinates the assembly of multiple DNA molecules into nucleoid-like structures. *Mol Biol Cell* 18:3225–3236
 50. Wang J, Silva JP, Gustafsson CM, Rustin P, Larsson NG (2001) Increased in vivo apoptosis in cells lacking mitochondrial DNA gene expression. *Proc Natl Acad Sci U S A* 98:4038–4043
 51. Naia L, Ribeiro MJ, Rego AC (2011) Mitochondrial and metabolic-based protective strategies in Huntington's disease: the case of creatine and coenzyme Q. *Rev Neurosci* 23:13–28
 52. Palazzolo I, Stack C, Kong L, Musaro A, Adachi H, Katsuno M, Sobue G, Taylor JP, Sumner CJ, Fischbeck KH, Pennuto M (2009) Overexpression of IGF-1 in muscle attenuates disease in a mouse model of spinal and bulbar muscular atrophy. *Neuron* 63:316–328
 53. Apostol BL, Illes K, Pallos J, Bodai L, Wu J, Strand A, Schweitzer ES, Olson JM, Kazantsev A, Marsh JL, Thompson LM (2006) Mutant huntingtin alters MAPK signaling pathways in PC12 and striatal cells: ERK1/2 protects against mutant huntingtin-associated toxicity. *Hum Mol Genet* 15:273–285
 54. Zala D, Colin E, Rangone H, Liot G, Humbert S et al (2008) Phosphorylation of mutant huntingtin at S421 restores anterograde and retrograde transport in neurons. *Hum Mol Genet* 17:3837–3846

55. Warby SC, Doty CN, Graham RK, Shively J, Singaraja RR et al (2009) Phosphorylation of huntingtin reduces the accumulation of its nuclear fragments. *Mol Cell Neurosci* 40:121–127
56. Metzler M, Gan L, Mazarei G, Graham RK, Liu L, Bissada N, Lu G, Leavitt BR, Hayden MR (2010) Phosphorylation of huntingtin at Ser421 in YAC128 neurons is associated with protection of YAC128 neurons from NMDA-mediated excitotoxicity and is modulated by PP1 and PP2A. *J Neurosci* 30:14318–14329
57. Havel LS, Wang CE, Wade B, Huang B, Li S et al (2011) Preferential accumulation of N-terminal mutant huntingtin in the nuclei of striatal neurons is regulated by phosphorylation. *Hum Mol Genet* 20:1424–1437
58. Gu X, Greiner ER, Mishra R, Kodali R, Osmand A et al (2009) Serines 13 and 16 are critical determinants of full-length human mutant huntingtin induced disease pathogenesis in HD mice. *Neuron* 64:828–840
59. Mishra R, Hoop CL, Kodali R, Sahoo B, van der Wel PC et al (2012) Serine phosphorylation suppresses huntingtin amyloid accumulation by altering protein aggregation properties. *J Mol Biol* 424:1–14
60. Sarkar S, Ravikumar B, Floto RA, Rubinsztein DC (2009) Rapamycin and mTOR-independent autophagy inducers ameliorate toxicity of polyglutamine-expanded huntingtin and related proteinopathies. *Cell Death Differ* 16:46–56
61. Gulati P, Gaspers LD, Dann SG, Joaquin M, Nobukuni T, Natt F, Kozma SC, Thomas AP, Thomas G (2008) Amino acids activate mTOR complex 1 via Ca²⁺/CaM signaling to hVps34. *Cell Metab* 7:456–465
62. Chiang GG, Abraham RT (2005) Phosphorylation of mammalian target of rapamycin (mTOR) at Ser-2448 is mediated by p70S6 kinase. *J Biol Chem* 280:25485–25490
63. Holz MK, Blenis J (2005) Identification of S6 kinase 1 as a novel mammalian target of rapamycin (mTOR)-phosphorylating kinase. *J Biol Chem* 280:26089–26093
64. Seong IS, Ivanova E, Lee J-M, Choo YS, Fossale E, Anderson M, Gusella JF, Laramie JM, Myers RH, Lesort M, MacDonald ME (2005) HD CAG repeat implicates a dominant property of huntingtin in mitochondrial energy metabolism. *Hum Mol Genet* 14:2871–2880
65. Wang H, Lim PJ, Karbowski M, Monteiro MJ (2009) Effects of overexpression of Huntingtin proteins on mitochondrial integrity. *Hum Mol Genet* 18:737–752
66. Koroshetz WJ, Jenkins BG, Rosen BR, Beal MF (1997) Energy metabolism defects in Huntington's disease and effects of coenzyme Q10. *Ann Neurol* 41:160–165
67. Panov AV, Gutekunst CA, Leavitt BR, Hayden MR, Burke JR, Strittmatter WJ, Greenamyre JT (2002) Early mitochondrial calcium defects in Huntington's disease are a direct effect of polyglutamines. *Nat Neurosci* 5:731–736
68. Josefsen K, Nielsen SM, Campos A, Seifert T, Hasholt L, Nielsen JE, Nørremølle A, Skotte NH, Secher NH, Quistorff B (2010) Reduced gluconeogenesis and lactate clearance in Huntington's disease. *Neurobiol Dis* 40:656–662
69. Martin WR, Wieler M, Hanstock CC (2007) Is brain lactate increased in Huntington's disease? *J Neurol Sci* 263:70–74
70. van der Burg JM, Bacos K, Wood NI et al (2008) Increased metabolism in the R6/2 mouse model of Huntington's disease. *Neurobiol Dis* 29:41–51
71. Powers WJ, Videen TO, Markham J, McGee-Minnich L, Antenor-Dorsey JV, Hershey T, Perlmutter JS (2007) Selective defect of in vivo glycolysis in early Huntington's disease striatum. *Proc Natl Acad Sci U S A* 104:2945–2949
72. Milakovic T, Quintanilla RA, Johnson GV (2006) Mutant huntingtin expression induces mitochondrial calcium handling defects in clonal striatal cells: functional consequences. *J Biol Chem* 281:34785–34795
73. Solans A, Zambrano A, Rodríguez M, Barrientos A (2006) Cytotoxicity of a mutant huntingtin fragment in yeast involves early alterations in mitochondrial OXPHOS complexes II and III. *Hum Mol Genet* 15:3063–3081
74. Benchoua A, Trioulier Y, Zala D, Gaillard MC, Lefort N, Dufour N, Saudou F, Elalouf JM, Hirsch E, Hantraye P (2006) Involvement of mitochondrial complex II defects in neuronal death produced by N-terminus fragment of mutated huntingtin. *Mol Biol Cell* 17:1652–1663
75. Ow YP, Green DR, Hao Z, Mak TW (2008) Cytochrome c: functions beyond respiration. *Nat Rev Mol Cell Biol* 9:532–542
76. Vempati UD, Han X, Moraes CT (2009) Lack of cytochrome c in mouse fibroblasts disrupts assembly/stability of respiratory complexes I and IV. *J Biol Chem* 284:4383–4391
77. Hayashi Y, Yoshida M, Yamato M et al (2008) Reverse of age-dependent memory impairment and mitochondrial DNA damage in microglia by an overexpression of human mitochondrial transcription factor a in mice. *J Neurosci* 28:8624–8634
78. Reijonen S, Putkonen N, Nørremølle A, Lindholm D, Korhonen L (2008) Inhibition of endoplasmic reticulum stress counteracts neuronal cell death and protein aggregation caused by N-terminal mutant huntingtin proteins. *Exp Cell Res* 314:950–960
79. Rosenstock TR, Brito OM, Lombradi V, Louros S, Ribeiro M, Almeida S, Ferreira IL, Oliveira CR, Rego AC (2011) FK506 ameliorates cell death features in Huntington's disease striatal cell models. *Neurochem Int* 59:600–609
80. Panov AV, Obertone T, Bennett-Desmelik J, Greenamyre JT (1999) Ca²⁺-dependent permeability transition and complex I activity in lymphoblast mitochondria from normal individuals and patients with Huntington's or Alzheimer's disease. *Ann N Y Acad Sci* 893:365–368
81. Rockabrand E, Slepko N, Pantalone A, Nukala VN, Kazantsev A, Marsh JL, Sullivan PG, Steffan JS, Sensi SL, Thompson LM (2007) The first 17 amino acids of Huntingtin modulate its sub-cellular localization, aggregation and effects on calcium homeostasis. *Hum Mol Genet* 16:61–77
82. Ibarra C, Estrada M, Carrasco L, Chiong M, Liberona JL, Cardenas C, Diaz-Arava G, Jaimovich E, Lavandero S (2004) Insulin-like growth factor-1 induces an inositol 1,4,5-triphosphate-dependent increase in nuclear and cytosolic calcium in cultured rat cardiac myocytes. *J Biol Chem* 279:7554–7565
83. Valdés JA, Flores S, Fuentes EN, Osorio-Fuentealba C, Jaimovich E, Molina A (2013) IGF-1 induces IP(3) dependent calcium signal involved in the regulation of myostatin gene expression mediated by NFAT during myoblast differentiation. *J Cell Physiol* 228:1452–1463
84. Steelman LS, Chappell WH, Abrams SL et al (2011) Roles of the Raf/MEK/ERK and PI3K/PTEN/Akt/mTOR pathways in controlling growth and sensitivity to therapy—implications for cancer and aging. *Aging (Albany NY)* 3:192–222